THEORETICAL AND EXPERIMENTAL STUDIES OF RADIATION-INDUCED DAMAGE TO SEMICONDUCTOR SURFACES AND THE EFFECTS OF THIS DAMAGE ON SEMICONDUCTOR DEVICE PERFORMANCE

Final Report On

NASA Grant NsG-588

1 September 1968

Semiconductor Device Laboratory
Department of Electrical Engineering
North Carolina State University
at
Raleigh, North Carolina

SDL-10-588

THEORETICAL AND EXPERIMENTAL STUDIES OF RADIATION-INDUCED DAMAGE TO SEMICONDUCTOR SURFACES AND THE EFFECTS OF THIS DAMAGE ON SEMICONDUCTOR DEVICE PERFORMANCE

Final Report On

NASA Grant NsG-588

1 September 1968

Semiconductor Device Laboratory
Department of Electrical Engineering
North Carolina State University
at
Raleigh, North Carolina

FOREWORD

This report was prepared by North Carolina State University, Raleigh, North Carolina, on National Aeronautics and Space Administration Grant NsG-588 "Theoretical and Experimental Studied of Radiation-Induced Damage to Semiconductor Surfaces and the Effects of this Damage on Semiconductor Device Performance". This work was administrated under the direction of Langley Research Center, Hampton, Virginia, with Mr. Chris Gross, technical monitor.

This report summarizes research efforts during the period March 1, 1964 to August 31, 1968. The work was performed in the Semiconductor Device Laboratory of the Electrical Engineering Department. R. W. Lade was principal investigator for the period March 1, 1964 to June 30, 1967, with J. R. Hauser assuming the role of principal investigator for the period July 1, 1967 to August 31, 1968. R. J. Mattauch, M. A. Littlejohn, F. J. Morris, C. L. Hutchins and J. R. Bridges also contributed significant work to the research performed under this grant.

ABSTRACT

This report summarizes the research performed under NASA Grant NsG-588, "Theoretical and Experimental Studies of Radiation-Induced Damage to Semiconductor Surfaces and the Effects of This Damage on Semiconductor Device Performance". The research efforts have been concentrated in five major areas. Details of the individual phases of this research have been reported in previous reports. The present report attempts to show how the individual research projects fit into the overall objectives of the research work and to summarize the most important findings of the research.

Two of the research projects were concerned with the measurement of surface potential, surface recombination velocity, and the effects of radiation on these parameters. A new technique employing an MOS field-effect solar cell has been demonstrated for simultaneously determining both surface potential and surface recombination velocity. Gamma irradiation was found to change the surface recombination through changes in both surface potential and in the density of recombination centers.

Three of the research projects were concerned with the properties and irradiation effects of semiconductors with silicon dioxide and silicon nitride insulating layers on the semiconductor. These properties were studied mainly by means of C-V measurements on metal-insulator-silicon devices. On SiO_2, the insulator charge changes and surface state density were studied for gamma irradiation. Silicon nitride insulator layers were found to be unstable because of an electronic injection from the semiconductor into the silicon nitride films. This effect was studied in detail and a model developed for this electronic type of instability.

Table of Contents

List of Figures

Figure Page

1. INTRODUCTION

The subject of radiation effects on semiconductor materials and devices has been of interest since the early days following the invention of the transistor. More recently the increased use of solid state devices in outer space and in nuclear environments has fostered additional work concerning the effects of all types of irradiation on solid state materials and devices. The majority of the early studies on radiation were in the areas of: 1) Investigation of bulk material variations (induced lattice defects densities as a function of integrated dosage, reduction of bulk minority carrier lifetime effects, etc.) and 2) Studies of terminal volt-ampere characteristic variations. The latter studies were generally an production line state-of-the-art devices.

Inprovements in solid state device technology within the past few years have made it possible to greatly reduce the physical size of solid state devices. With this size reduction, the semiconductor-surface interface has taken on a much more significant role in determining device performance. The Metal-Oxide-Semiconductor device relies completely on a thin conductive channel of charge at the semiconductor surface for its operation. These trends made it apparent at the beginning of this research that radiation effects to semiconductor surfaces and to any insulating layers on the semiconductor were becoming as important or more important than bulk radiation damage in determining device degradation in a radiation environment. At the initiation of the study little was known about the effects of radiation on surface recombination and on oxide-semiconductor interfaces. Through the research supported by NASA in this study and through the research of other organizations, much is now known about the effects of radiation on surface recombination, and on semiconductor-insulator interfaces.

There are a wide range of possible sources which can be used to study radiation effects. Electrons, protons, and gamma rays are the most common types of radiation. For the purposes of the present work it was decided to concentrate on irradiation damage due to gamma rays. There were several reasons for this. First, a gamma irradiation source was conveniently available for these studies. More importantly, however, is the fact that gamma irradiation results are easier to interpret than irradiation results with charged particles. Charged particles such as electrons or protons not only produce irradiation damage, but they also directly add charges to the material under study. This is particularly important for surface studies, because irradiation electrons can become trapped within an oxide insulating layer on silicon and remain trapped for extended periods of time. This complicates the interpretation of experimental results because one has not only irradiation damage but also an effect due to trapped irradiation charges.

The irradiation used in this work was supplied by Cobalt-60 gamma rays from a "Gammacell 220" manufactured by Atomic Energy of Canada Limited. The normalized spectrum of the energy in the sample chamber of the Gammacell is shown in Figure 1. The exposure dose rate was approximately 2×10^5 roentgens/hr, which corresponds to a photon flux of approximately 10^{11} photons/cm^2/sec. For the Gammacell photons, with a mean energy of 1.25 MeV, and for Silicon, with an atomic number of 14, the Compton effect is the dominant mechanism by which gamma rays interact with the semiconductor [1].

During the early phases of this work on radiation damage to semiconductor surfaces, it became apparent that it is difficult to separate surface effects completely from effects which are occuring within any insulating layer on the semiconductor. Surface properties such as surface

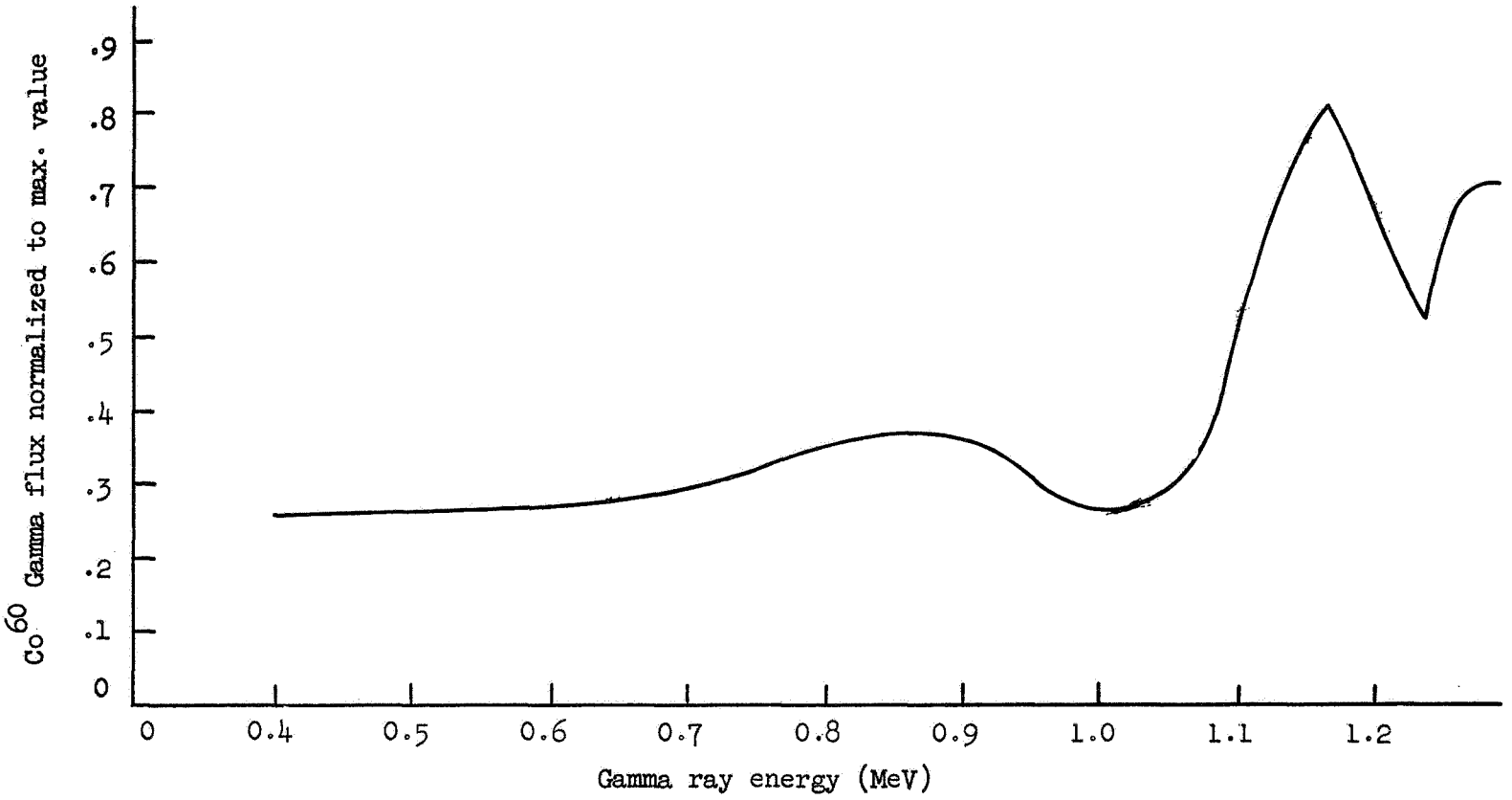

Figure 1. Normalized primary photon flux as a function of energy in the sample chamber of the Gammacell 220 (Source: Atomic Energy of Canada, Ltd., Ottawa, Canada)

recombination, and surface state charge are drastically influenced by the properties of any insulating layer on the semiconductor. They are influenced not only by the chemical and physical properties of the interface region between the insulator and semiconductor, but they are also influenced by charges within the insulating layer. Surface properties are thus greatly influenced by the insulating layer properties, and in many cases changes in surface properties from irradiation are determined almost entirely by irradiation effects on the insulating layer. The bulk of the present research has been done on silicon with SiO_2 and Si_3N_4 as the insulating layers.

The importance of the insulating layer became apparent from studies of the effects of gamma irradiation on steam-grown SiO_2, MOS devices, and also from studies of the effects of gamma irradiation on bulk and surface recombination rates. Consequently much of the later research effort under this grant has been directed at studying the properties of insulating layers of SiO_2 and Si_3N_4 on silicon. A reasonably consistent picture of irradiation effects has now been obtained for SiO_2 insulated semiconductor regions. For silicon nitride films however, we are just beginning to understand the instabilities present with these films and hopefully to understand how to avoid these instabilities in insulating layers on semiconductors.

This research grant has provided complete support for the Ph.D. research work of four graduate students and partial support for one other student. Thesis topics for these five students are listed below:

1. "A Study of the Effects of Co^{60} γ-Radiation on Steam-Grown SiO_2 MOS Structures," R. J. Mattauch, 1966.
2. "Influence of Co^{60} Gamma Irradiation on the Bulk and Surface Recombination Rates in Silicon", M. A. Littlejohn, 1967.

3. "A Study of the Effects of the Surface Potential on the Surface Recombination Velocity at a Silicon-Silicon Oxide Interface," F. J. Morris, 1967.
4. "Charge Transients in Aluminum-Silicon Nitride-Silicon Capacitors," C. L. Hutchins, 1968.
5. "Electronic Instabilities in Metal-Insulator-Semiconductor Devices", J. R. Bridges, work still in progress.

The majority of the research activity under this grant has been centered around these five areas.

2. SUMMARY OF RESEARCH PROJECTS

The details of the research performed under NASA Grant NsG-588 are much too lengthy to be contained in a single report. These details are contained in five previous reports [2] [3] [4] [5] [6]. The present chapter summarizes the major results of these phases of the work. The reader is referred to the previous reports for details of the research.

2.1. The Effects of Co^{60} γ-Radiation on Steam-Grown SiO_2 MOS Structures [2] [7]

This is the initial research project undertaken on this grant. The object of the research was to study the effects of Co^{60} gamma irradiation on thermally grown steam oxides. At the initiation of the study there was vigorous research activity on the bias instability present in thermal oxides, and the origin of this ionic instability had not been completely established. Basically this phase of the research consisted of the fabrication of steam oxide MOS devices, and the study of these devices as to ionic instability and as to the effects of gamma irradiation on the devices. The steam oxides were grown in a conventional resistance heated furnace using distilled and deionized water as the source for the steam. Aluminum gate electrodes were applied to the oxide, and the devices were finally mounted on TO-5 headers for study.

The quality and properties of the devices were studied by observing the capacitance-voltage characteristics of the devices. Capacitance data was obtained either by point-by-point measurements on a capacitance bridge or by an x-y recorder using an unbalanced bridge as an indication of the capacitance.

Typical capacitance-voltage characteristics for the devices produced are shown in Figure 2. The curves illustrate the ionic instability present in the devices studied*. Curve (1) for the negative saturation position represents the limiting position of the C-V curve after a large negative bias has been applied for a long time. For such a large negative gate bias, positive ions within the oxide accumulate at the metal gate electrode and have little influence on a rapidly measured C-V curve. Curves (2) through (5) correspond to a drift of positive ions in the oxide toward the oxide-semiconductor interface following the application of a positive bias. This behavior is typical of that observed by many investigators [8] [9]. The activation energy for the positive ion drift was found to be very near that of sodium in fused silicon.

The effect of gamma radiation on the C-V curve for an MOS device on p-type silicon is shown in Figure 3. The increasing numbers with the curves corresponding to increasing gamma radiation as given in Table 1. There are two features of the curves of Figure 3. First, there is a shift of the C-V curve toward more negative bias voltages with increasing radiation. This indicates a net increase in the positive charge within the oxide. Second, there is a changing slope on the C-V curves with increasing radiation, i.e., the transition from maximum to minimum capacitance is more gradual with increasing radiation. This indicates an increase in the density of fast interface states with radiation.

---

*For a complete discussion of the various types of instabilities present in metal-insulator-semiconductor devices see Reference 6.

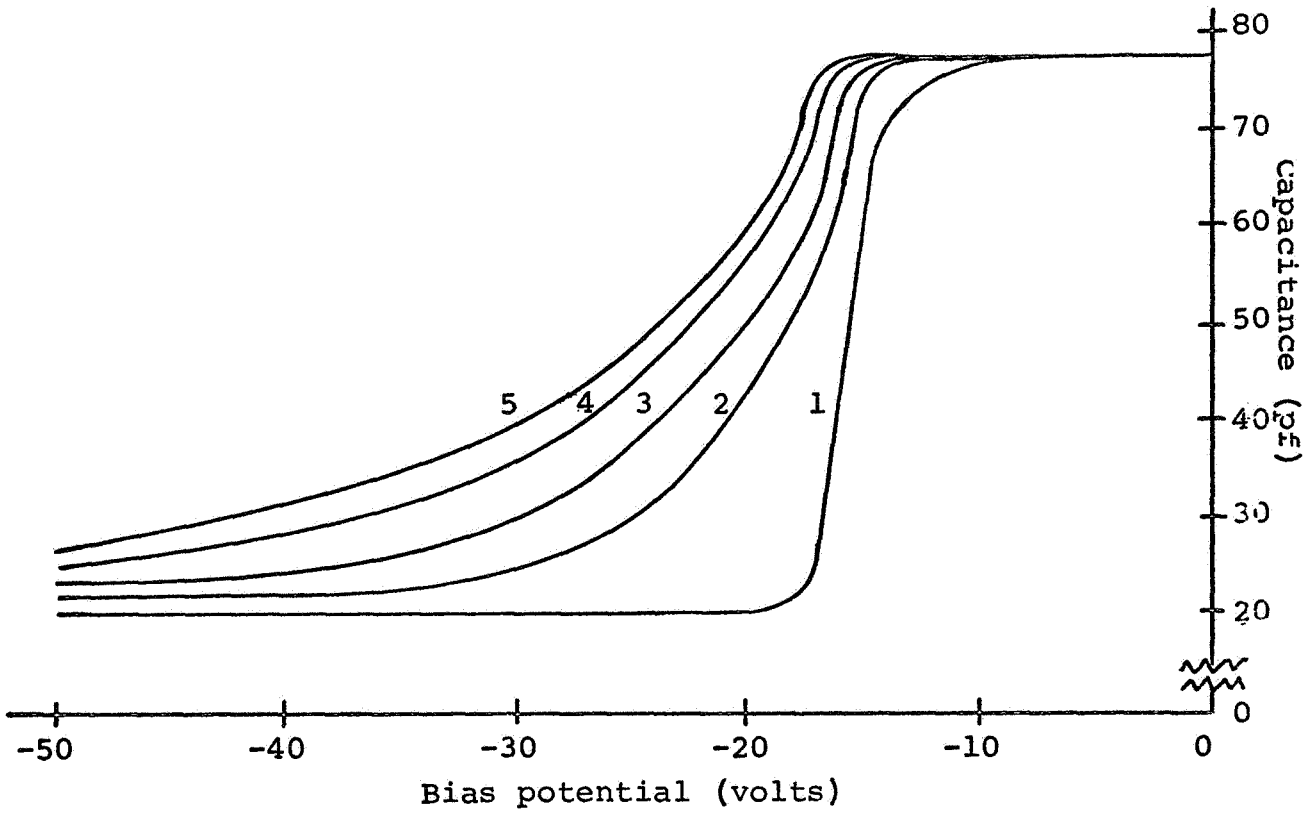

Figure 2. Capacitance-bias voltage curves for n-type device, number 14-33: curve (1) is in the negative saturation position while curves (2) through (5) were taken after one 10 minute and three 20 minute, 62°C, +3.0 volt anneals respectively

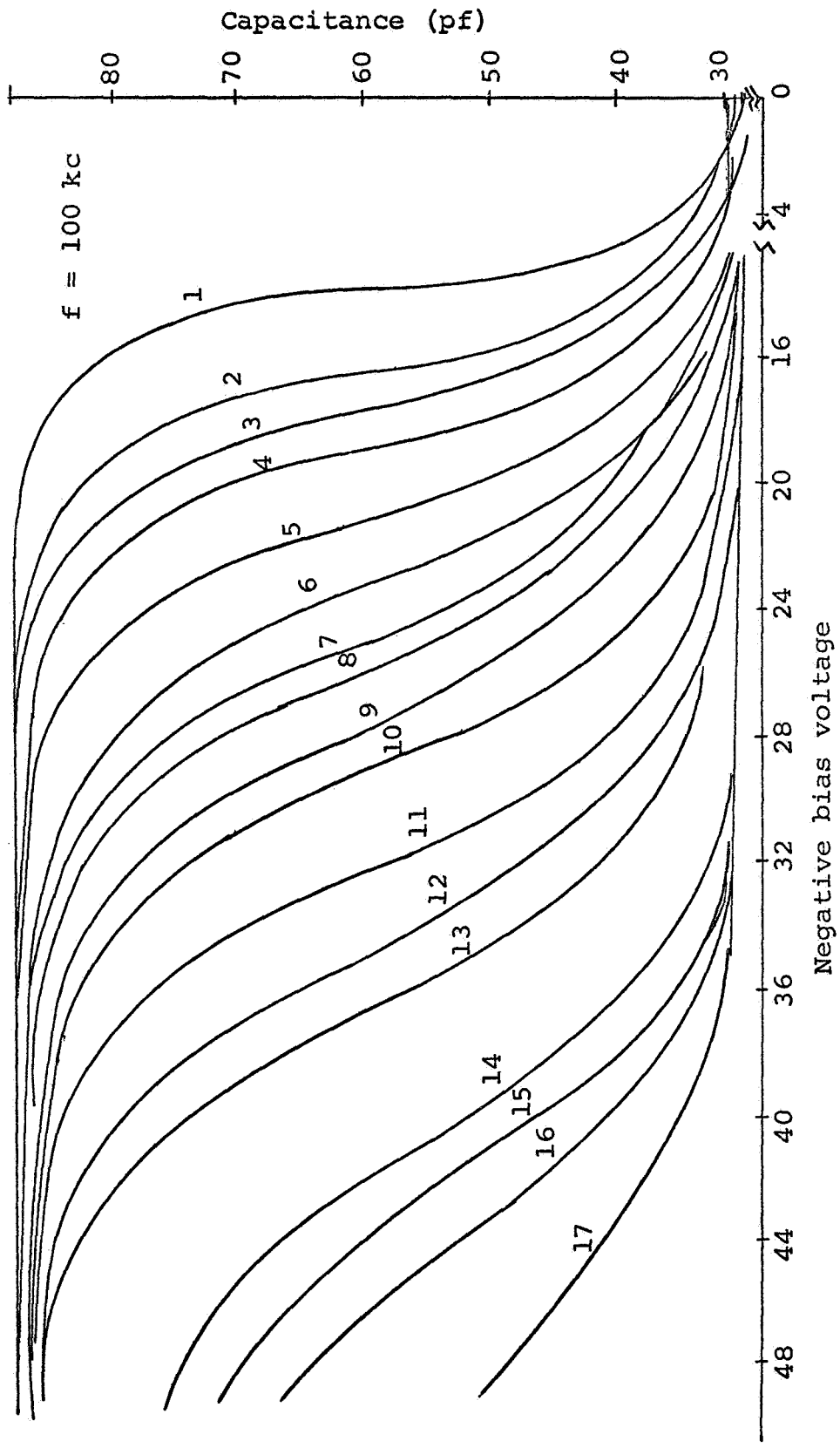

Figure 3. Point-by-point capacitance-bias voltage curves for p-type device number 36-44 showing shift of curves toward more negative bias with increasing gamma radiation as given in Table 1

Table 1. Co^{60} Radiation information for p-type device number 36-44.

CV curve taken after irradiation	Time of irradiation (minutes)	Exposure (roentgens)	Total exposure
1	0	0	0
2	15	$.5 \times 10^5$r	$.5 \times 10^5$r
3	15	$.5 \times 10^5$r	1.0×10^5r
4	15	$.5 \times 10^5$r	1.5×10^5r
5	30	1.0×10^5r	2.5×10^5r
6	30	1.0×10^5r	3.5×10^5r
7	30	1.0×10^5r	4.5×10^5r
8	30	1.0×10^5r	5.5×10^5r
9	30	1.0×10^5r	6.5×10^5r
10	30	1.0×10^5r	7.5×10^5r
11	60	2.0×10^5r	9.5×10^5r
12	60	2.0×10^5r	11.5×10^5r
13	60	2.0×10^5r	13.5×10^5r
14	120	4.0×10^5r	17.5×10^5r
15	120	4.0×10^5r	21.5×10^5r
16	120	4.0×10^5r	25.5×10^5r

Similar curves for an MOS device on n-type silicon are shown in Figure 4. Similar trends are observed for this device as for the p-type device. These features are a shift of the C-V curves toward more negative gate voltages indicating a increase of positive charge in the oxide, and a decrease in slope of the C-V curve indicating an increase in surface state density with radiation.

The surface state density as a function of surface potential is shown for the two devices in Figures 5 and 6. These surface state density calculations were carried out on the basis of the method of Zaninger and Warfield [10]. The gamma radiation is seen to have increased the surface state density by about an order of magnitude from $10^{11}/cm^2$-ev to $10^{12}/cm^2$-ev after an exposure of 3.6×10^6 roentgen. It was found that the radiation induced increase in surface state density could be essentially eliminated by annealing the devices at 75°C for 15 minutes with a -3.0 volt bias. The results obtained in this phase of the work are consistent with irradiation results obtained by other researchers on oxide devices.

Annealing experiments also indicated an interesting effects of radiation on the non-driftable charge within the oxide. By applying a negative gate bias for an extended period of time, the mobile ionic charge within the oxide is drifted to the metal interface. At this point it makes little contribution to the flat band voltage. When this is accomplished, oxide devices still generally have a net positive oxide charge. The origin of this charge is somewhat uncertain although silicon ions have been postulated as the charge species [11].

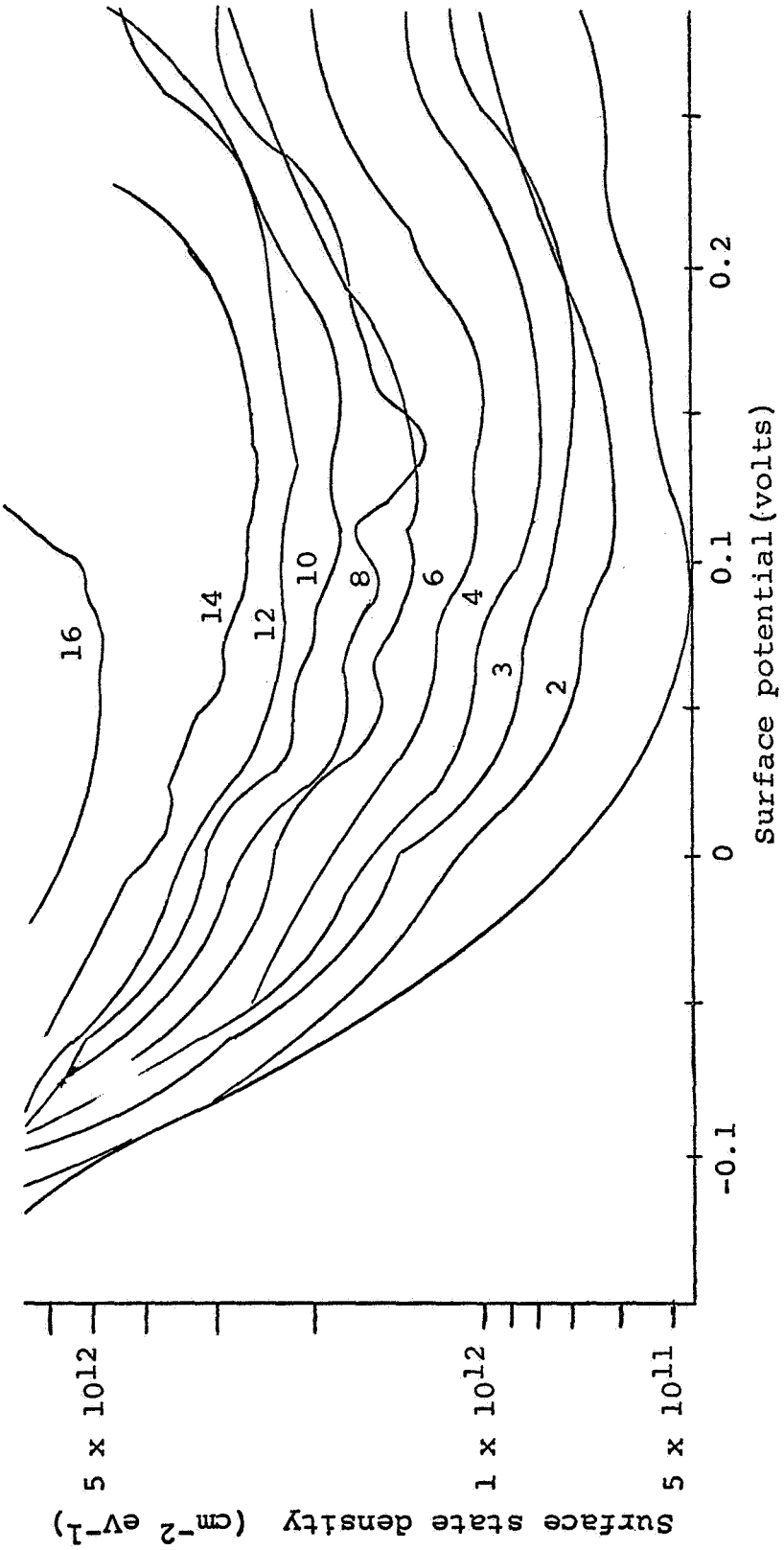

Figure 4. Curves of surface state density versus surface potential for increasing gamma irradiation of device number 36-44 as given in Table 1

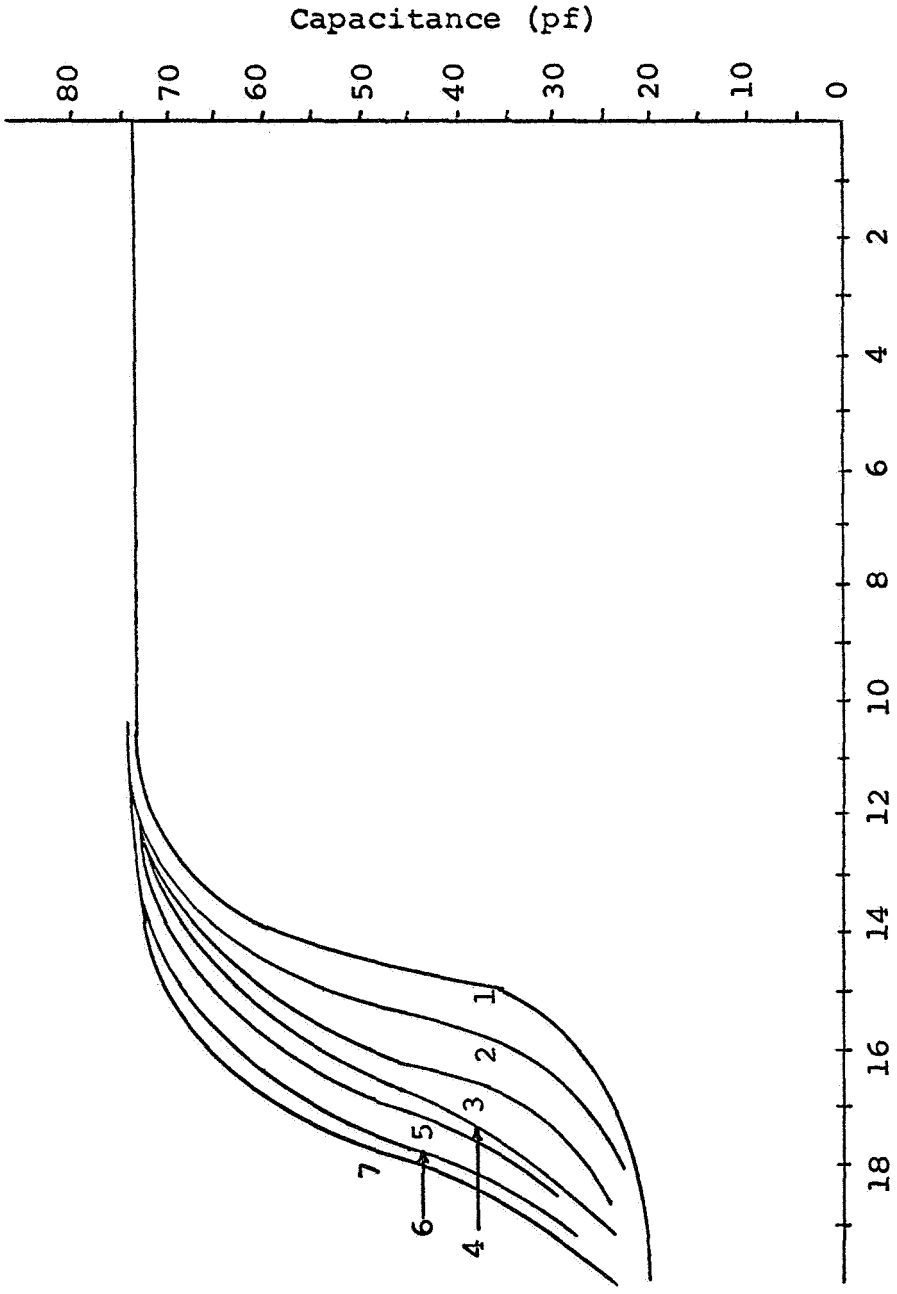

Figure 5. Point-by-point capacitance-bias voltage curves for n-type device number 14-43 showing shift of curves toward more negative bias with increasing gamma radiation as given in Table 2

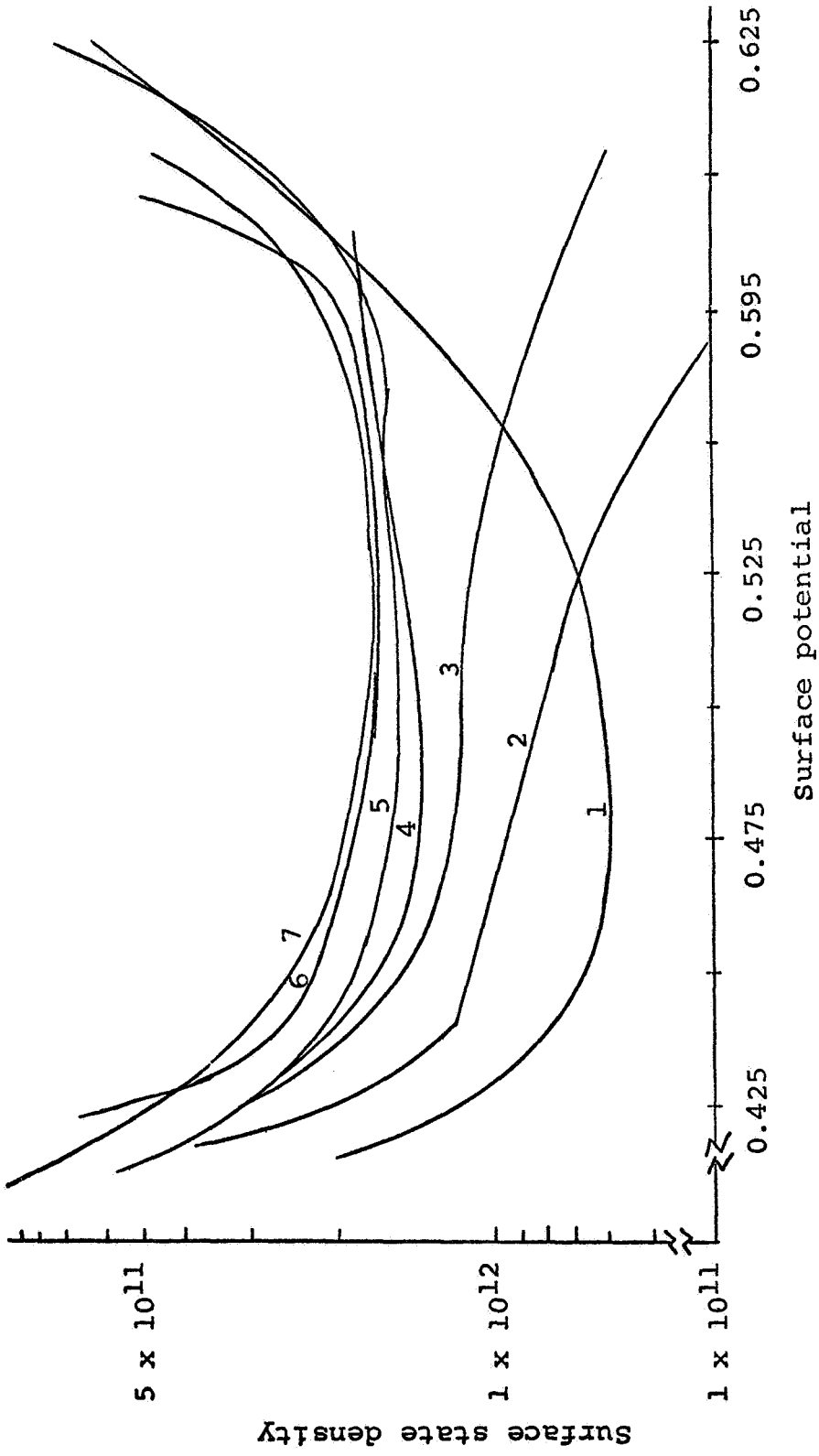

Figure 6. Curves of surface state density versus surface potential for increasing gamma irradiation of device number 14-43 as given in Table 2.

Table 2. Co^{60} radiation information for n-type device number 14-45.

CV-curve taken after exposure	Time of irradiation (minutes)	Exposure (roentgens)	Total exposure
1	0	0	0
2	15	$.5 \times 10^5$r	$.5 \times 10^5$r
3	15	$.5 \times 10^5$r	1.0×10^5r
4	30	1.0×10^5r	2.0×10^5r
5	15	$.5 \times 10^5$r	2.5×10^5r
6	15	$.5 \times 10^5$r	3.0×10^5r
7	45	1.5×10^5r	4.5×10^5r

The effect of radiation on this immobile positive charge is shown in Figure 7. The negative saturation curves are simply the C-V curve after all mobile ionic charge is drifted to the gate electrode. After irradiation, the device was annealed at 75°C with a -3.0 volt bias for 10 minutes and then the C-V curve shown in Figure 7 taken. Irradiation times are given in Table 3. Irradiation is seen to produce a very significant reduction in the non-driftable component of oxide charge. This is in sharp contrast to the shift of the C-V curves following irradiation and without the high temperature, negative bias annealing procedure.

The work performed in these experiments and the work of other investigators has now provided a fairly complete picture of gamma irradiation effects on steam oxide MOS devices.

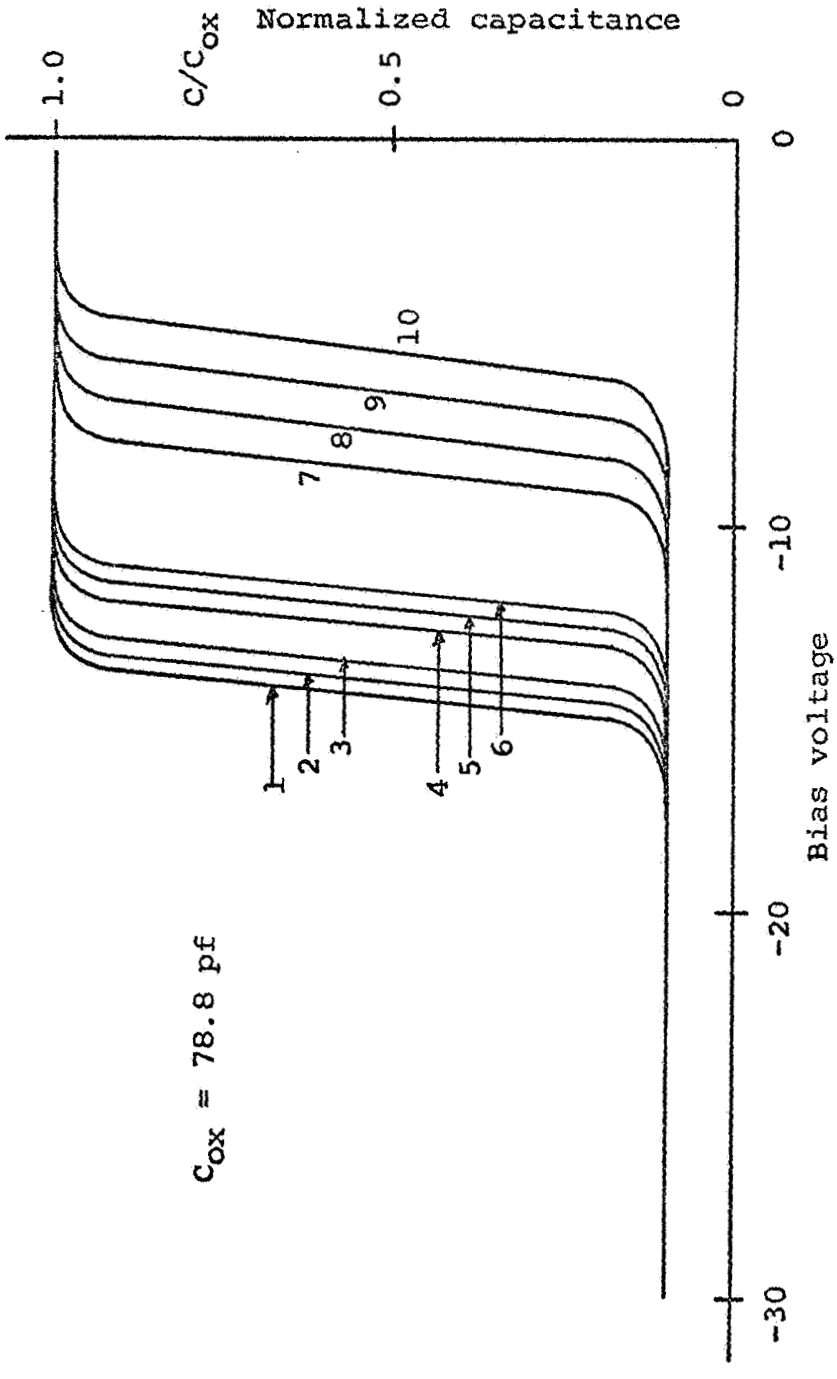

Figure 7. Negative saturation capacitance-bias voltage curves: curve (1) was taken prior to irradiation while curves (2) through (10) were taken after irradiation periods as shown in Table 3

Table 3. Co^{60} irradiation information for device 14-41: see Figure 7. for device curves

CV-curve taken after irradiation	Time of irradiation (minutes)	Exposure (roentgens)	Total exposure
1	0	0	0
2	1	1.97×10^3	1.97×10^3
3	2	3.44×10^3	5.37×10^3
4	3	5.91×10^3	1.12×10^4
5	2	3.44×10^4	1.47×10^4
6	2	3.44×10^3	1.81×10^4
7	60	2.00×10^5	2.18×10^5
8	470	1.57×10^6	1.78×10^6
9	600	2.00×10^6	3.78×10^6
10	720	2.40×10^6	6.18×10^6

2.2. The Influence of Co^{60} Gamma Irradiation on the Bulk and Surface Recombination Rates in Silicon [3] [12]

At the beginning of this research, the effects of radiation on bulk recombination rates had been studies, but little was known about the effects of radiation on surface recombination rates. Silicon was chosen as the material to study because of its dominant use in semiconductor devices. The technique of photoconductive decay in rectangular semiconductor filaments was used to measure the bulk and surface lifetime and surface recombination velocity of 100 ohm-cm n-and p-type float zone refined silicon doped with phosphorus and boron respectively.

Surface and bulk contributions to filament lifetime were separated through the use of samples which were similar with respect to bulk properties but which had different surface treatments. The surfaces of the bars which were used for surface lifetime measurements were chemically polished with an etch solution consisting of 90% hydroflouric acid and 10% nitric acid. The normal etching time was ten minutes.

A diagram of the experimental setup used to measure lifetime by the photoconductive decay technique is shown in Figure 8. The exponential generator generates an exponentially decaying voltage of known time constant. This is compared with the signal from the silicon sample, and the time constant of the exponential generator adjusted until the two signals have the same decay constant. The lifetime is then equal to the time constant of the exponential generator signal. This technique has been found to be a very convenient and reliable technique for lifetime measurements.

In studying surface lifetime a careful examination was made of the normal model of surface recombination at a discrete surface level and in the basic definition of surface lifetime. When space charge regions are located at semiconductor surfaces, it was found that there is a contribution to surface lifetime in addition to the normal recombination at surface states. This arises because of recombination within the surface space charge region, and the effect is especially significant when there is a depletion and possible an inversion layer at the surface. The effect is similar to recombination within the depletion region of a p-n junction. Surface recombination can be written as

$$S = S_o + S_r, \tag{1}$$

where S_o is the normal surface recombination velocity and S_r is the contribution from recombination within the space charge region. A sketch of

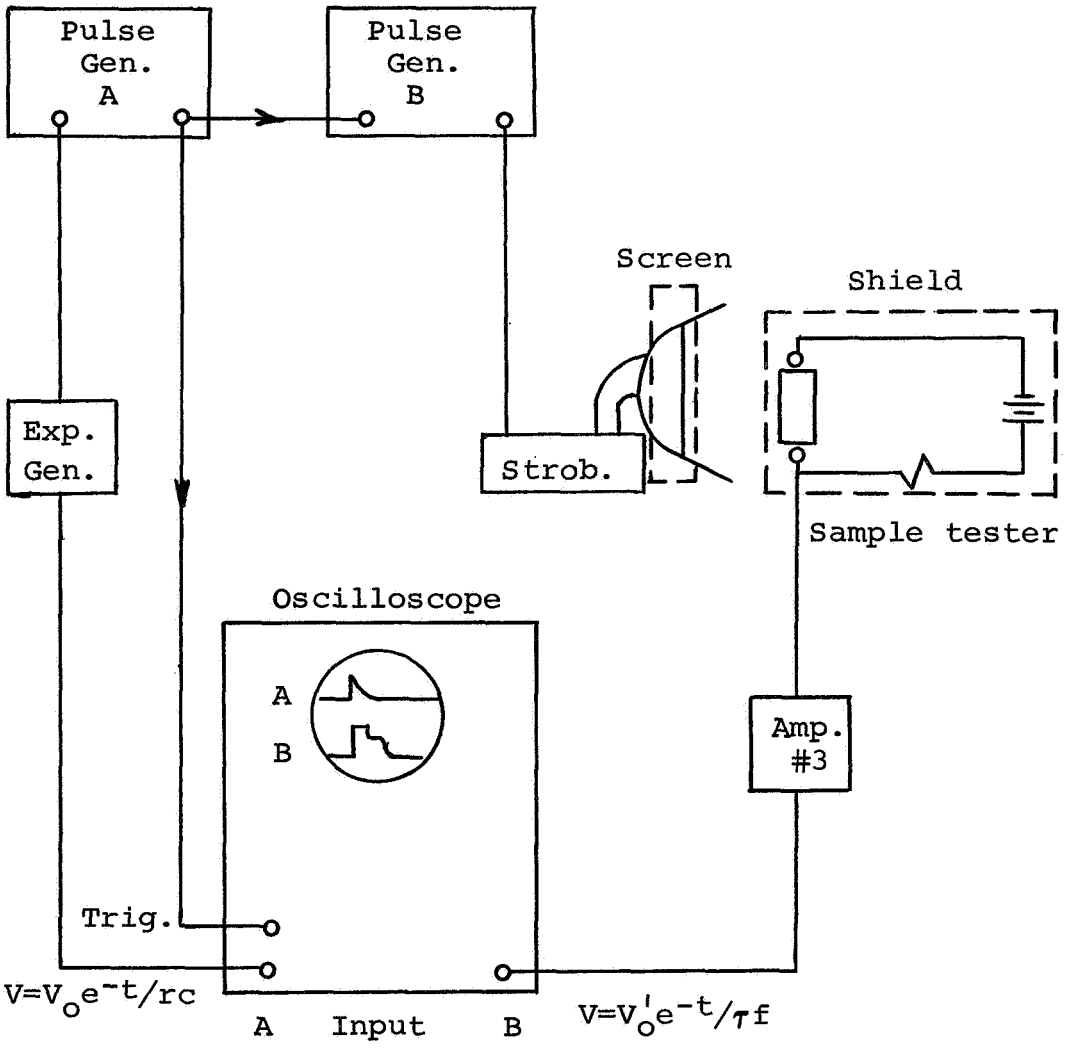

Figure 8 Lifetime measurement apparatus

the total surface recombination velocity as a function of normalized surface potential ($U_s = qV_s/kT$) is shown in Figure 9. The quantity S_r approaches zero as k approaches zero as seen in the figure. Contributions from space charge recombination has not been recognized by many investigators.

In this work bulk lifetime was found to decrease in irradiated material in a manner similar to that observed by other investigators [3]. Typical data are shown in Figure 10 as a function of reciprocal temperature and at various irradiation levels. The solid curves are computer fits to the normal, single level Schokley-Read model.

The changes in surface recombination velocity as a function of gamma ray exposure time are shown in Figures 11 and 12 for n- and p-type material respectively. Surface lifetime is observed to initially decrease and then increase for n-type material with increased irradiation time, while for p-type material there is only a slight increase in surface recombination velocity with increasing irradiation time. Typical experimental data for surface lifetime as a function of reciprocal temperature and at various irradiation times are shown in Figure 13. The solid lines are computer curve fits to a single level recombination model for surface recombination.

The changes in surface recombination velocity as shown in Figures 11 and 12, have been explained qualatively by the model shown in Figure 9. This figure shows that S depends on surface potential as well as the other material parameters of the semiconductor. It is also known that irradiation can change the effective surface state charge of a semiconductor and thus change the surface potential. The initial decrease in surface recombination velocity with irradiation for n-type material strongly suggests

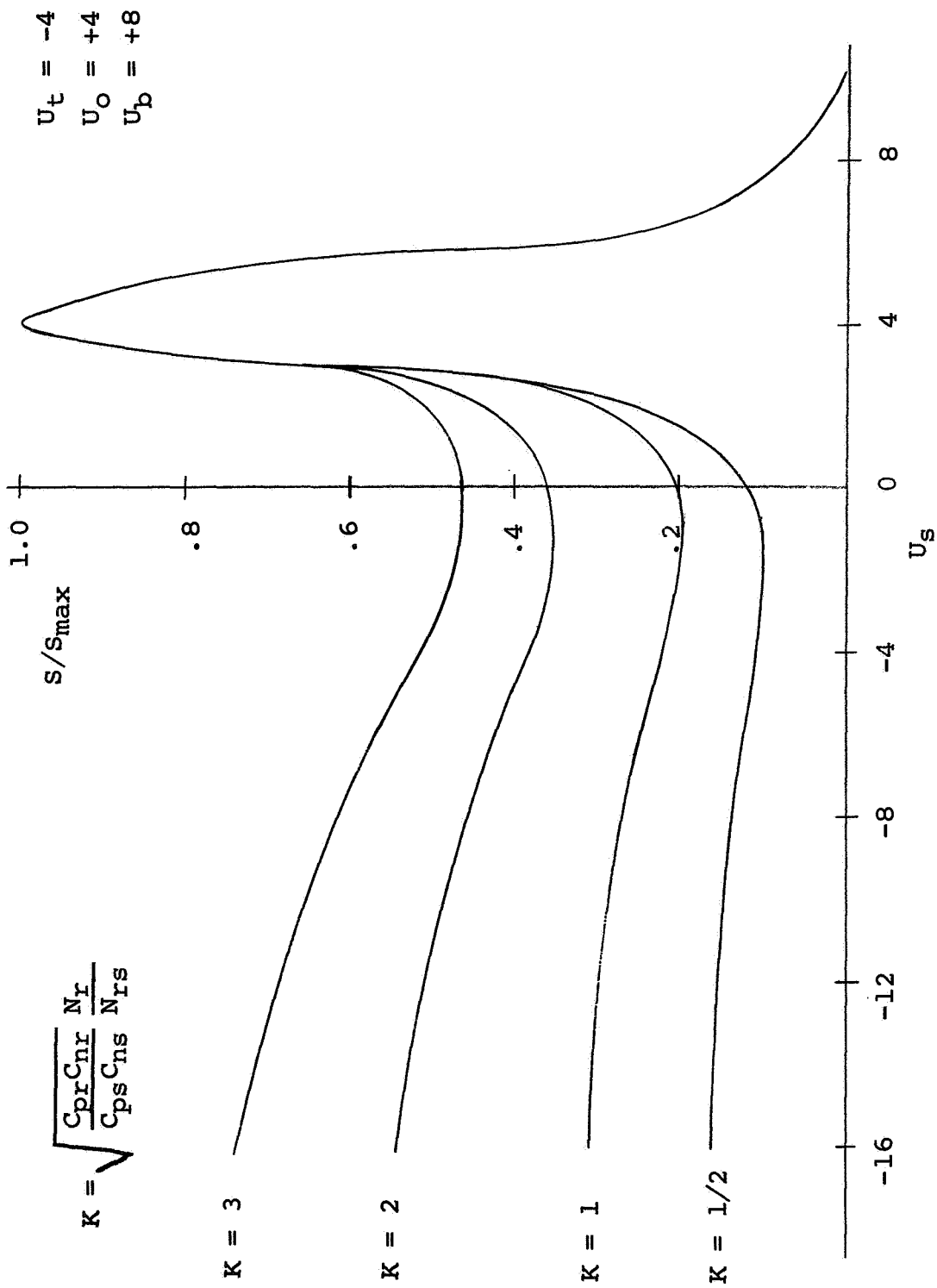

Figure 9 Surface recombination velocity vs. surface potential including recombination in the space charge region

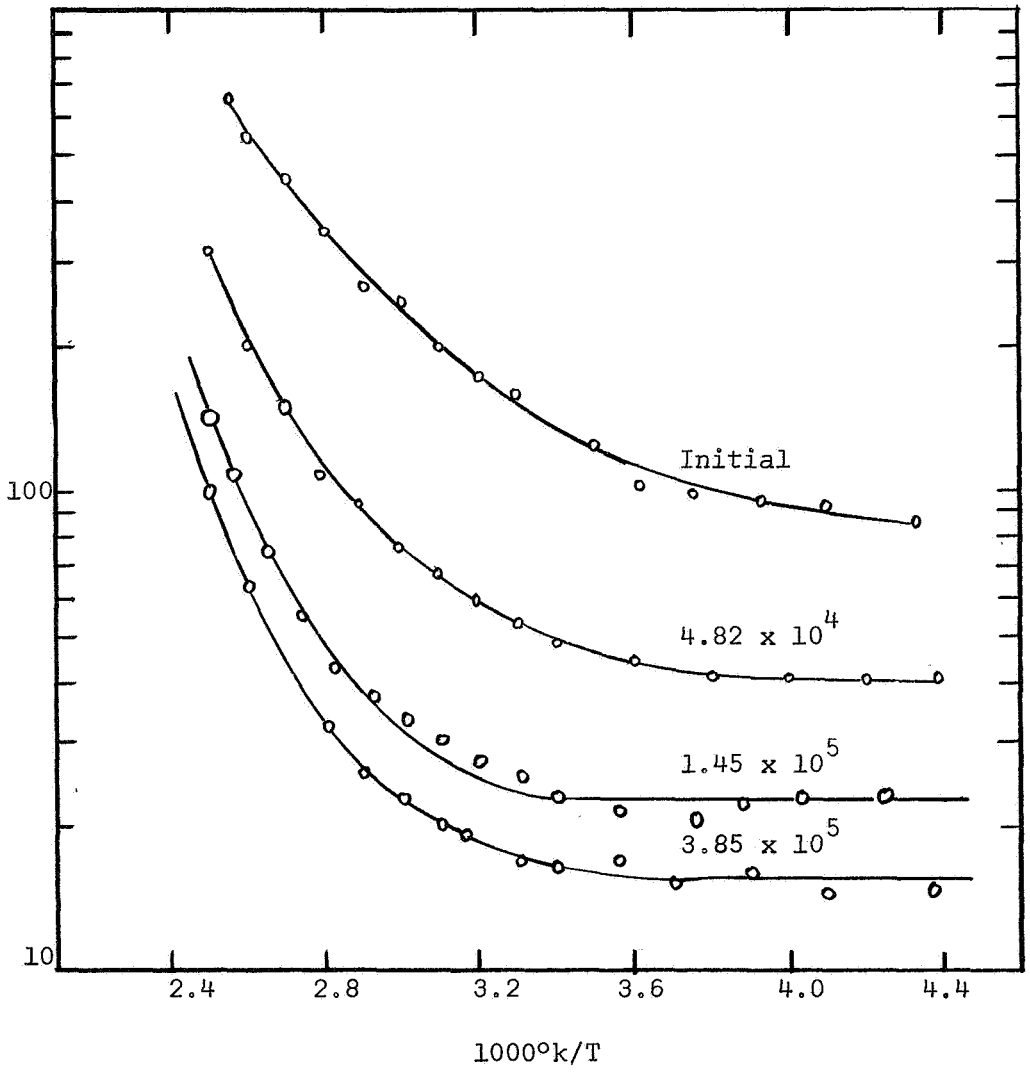

Figure 10. Bulk lifetime vs. reciprocal temperature for sample INA58-7. Values on the curves are gamma ray exposure in roentgens.

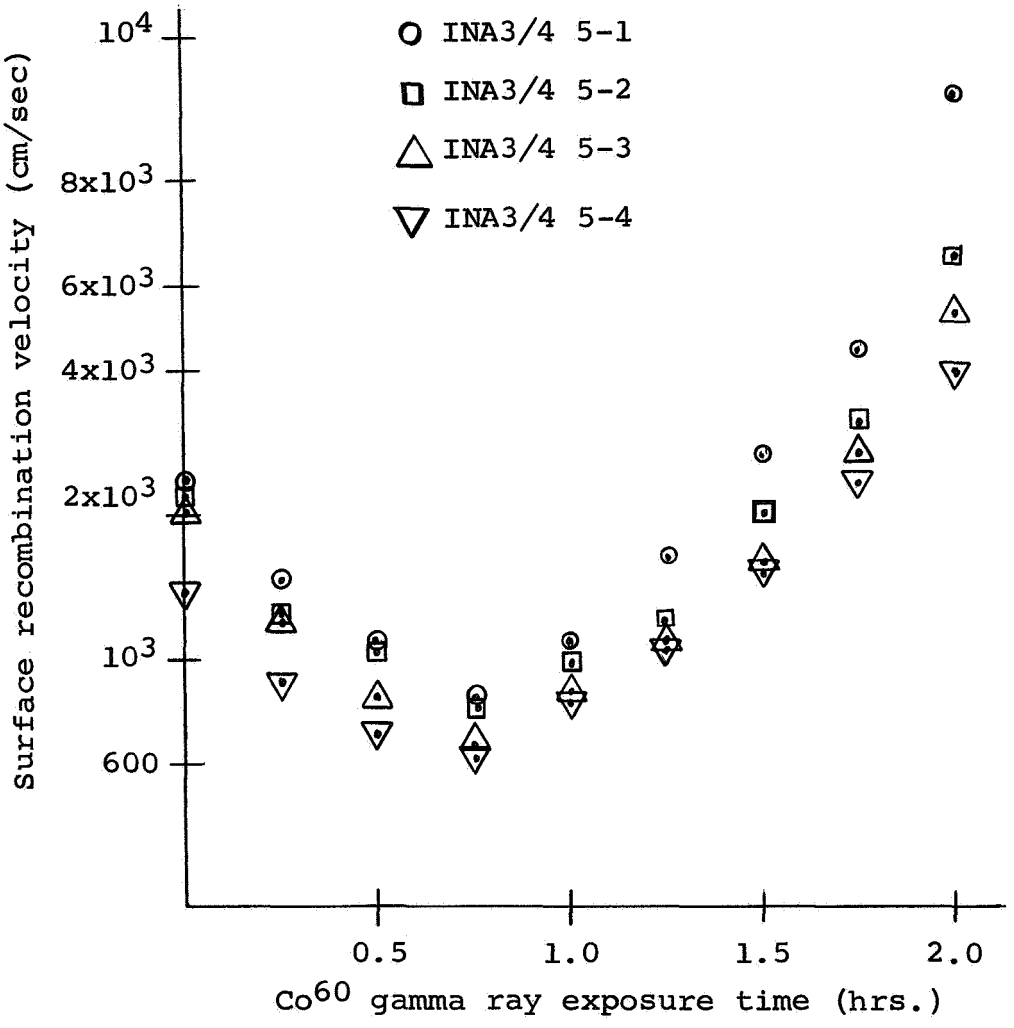

Figure 11 Surface recombination velocity vs. gamma ray exposure time. The exposure rate is 1.94×10^5 roentgens per hour

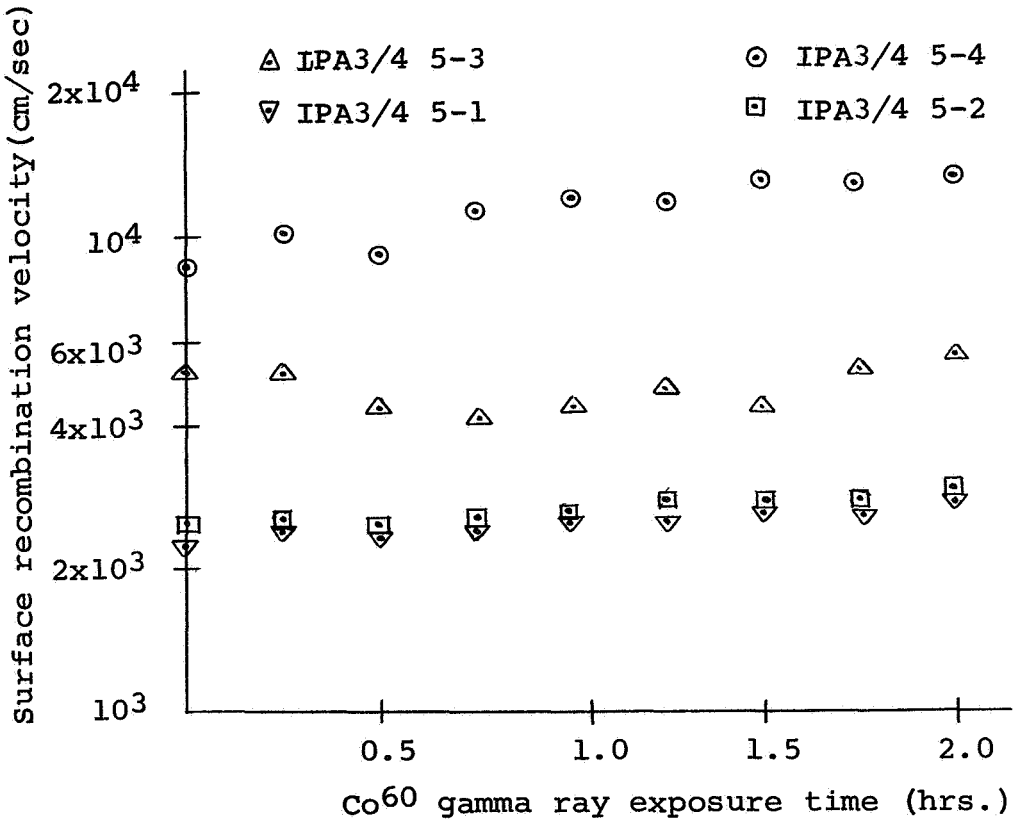

Figure 12 Surface recombination velocity vs. gamma ray exposure time for four p-type samples. The exposure rate is 1.94×10^5 roentgens per hour

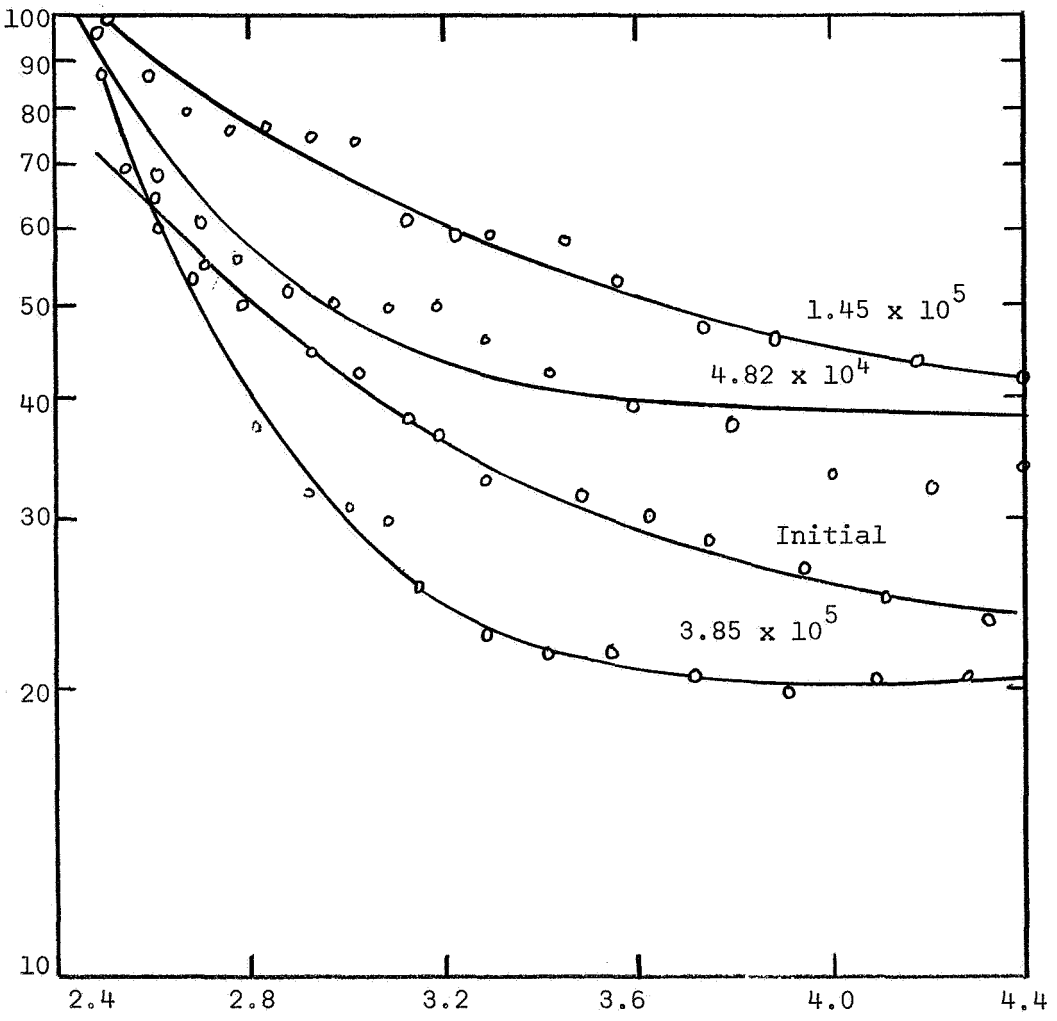

Figure 13. Surface lifetime vs. reciprocal temperature for sample INA3/4-1/ Values on the curves are gamma ray exposure in roentgens.

that surface potential changes with irradiation are playing a strong part in the observed changes in surface recombination. Radiation should cause, if anything, an increase in the density of surface recombination sites and this alone can only lead to an increase in surface recombination velocity. Also, changes in surface potential of only a few kT/q can cause rather large changes in surface recombination. Thus it is concluded that the changes in surface potential due to irradiation are largely responsible for the observed changes in surface recombination velocity. This model is qualitatively in agreement with the observations for both n- and p-type material if it is assumed that the surface potential becomes more negative under irradiation. This hypothesis could not be directly tested using the photoconductive decay aparatus.

The recombination center which dominates the bulk lifetime in n-type material was found to be different from the one which controls the lifetime in p-type material. In n-type material the recombination center created by gamma radiation was found to be located at 0.40 ev below the conduction band edge and is associated with a phosphorus-vacancy complex in the crystal. In p-type material, the center was found to be located at 0.18 ev above the valence band edge. It is believed that this is the first time such a recombination center has been observed in p-type float zone refined material.

The temperature variation of surface lifetime obeyed the one-level Shockley-Read equation for lifetime. No single energy level could be located at the surface, however, since the position of this level changed with each additional exposure to gamma radiation. For both types of material the location of the surface recombination level was nearly the

same with respect to the band edges, being approximately 0.25 ev above the valence band for n-type material and approximately 0.2 ev below the conduction band for p-type material.

2.3. The Effects of the Surface Potential on the Surface Recombination Velocity at a Silicon-Silicon Oxide Interface [4]

The work on surface recombination described in the previous section gave rise to two questions which were investigated in this phase of the research. The experimental evidence indicated that irradiation effects on surface recombination were greatly influenced by surface potential changes due to the irradiation. The photoconductive decay technique did not permit a unique determination of the relative importance of surface potential changes as opposed to radiation induced surface recombination levels. In addition, the work was done on unpassivated silicon samples while most present day devices have an insulating layer of silicon dioxide on the surface. Surface recombination would not be the same for chemically polished surfaces and surfaces with a thermally grown oxide.

Thus a research project was undertaken with the objective of developing a technique for simulataneously measuring both surface potential and surface recombination velocity. This was accomplished through the use of an MOS, field-effect solar cell. A sketch of this device is shown in Figure 14. The structure is a combination MOS device and a solar cell. The gate of the MOS device has a fairly transparent electrode of aluminum. Light passing through the gate produces hole-electron pairs in the semiconductor and part of these carriers can be collected by the p-n junction which functions as a solar cell. The semiconductor region consisted of a 10 ohm-cm 0.5 mil thick, epitaxial p-type layer on a 0.02 ohm-cm n-type substrate.

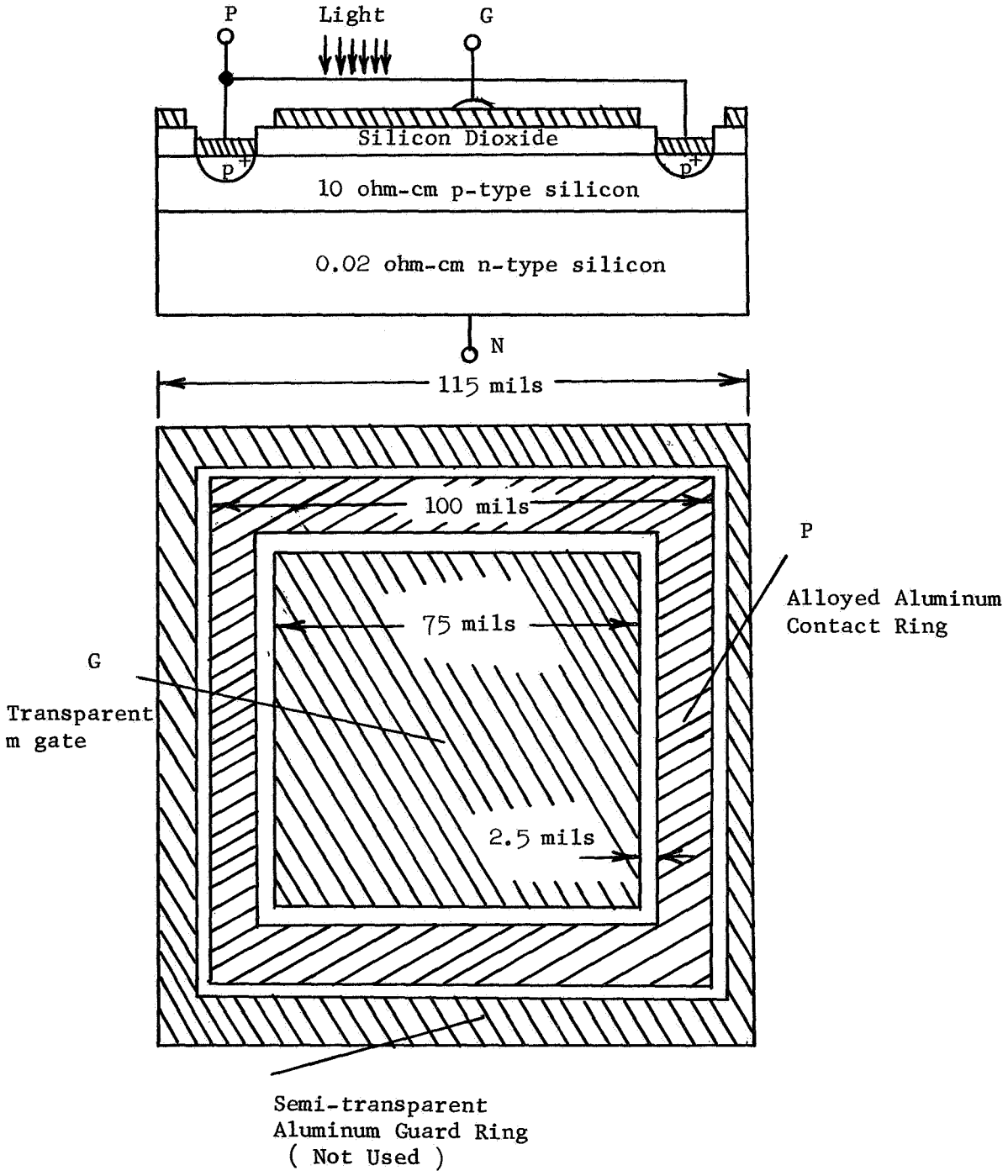

Figure 14 Sketch of a field effect device for determining the surface recombination velocity versus surface potential at the silicon-silicon dioxide interface

The basic idea of the MOS solar cell is that at any given gate voltage one can measure both the MOS capacitance and the short circuit current of the p-n junction. The short circuit current is influenced by any surface recombination, so surface recombination can be determined from the current measurements. The corresponding surface potential can be determined from MOS capacitance measurements. Thus surface recombination can be determined as a function of surface potential.

During the course of the research, additional studies were carried out on the theory of surface recombination. A theoretical model for the short circuit current for the MOS solar cell was developed in terms of the surface recombination velocity. Studies were also continued on the effect of a surface space charge region on surface recombination as well as studies of the effects of excess carrier densities on surface recombination. In addition, a model for surface recombination for surface states distributed in energy at the surface was studied. This work provides much additional insight into surface recombination. Details of this work are contained in Reference 4. Figure 15 shows one example of this work which is the variation of surface recombination velocity with surface potential for a uniform distribution of recombination levels. As shown in the figure, rather low values of excess carrier density can result in rather large reductions in the surface recombination velocity.

Many devices with the geometry shown in Figure 14 were built and experimentally investigated. They were constructed on epitaxial p-n wafers which were commercially purchased. Standard oxidation, metalization, alloying, and photoresist techniques were used in processing of the devices.

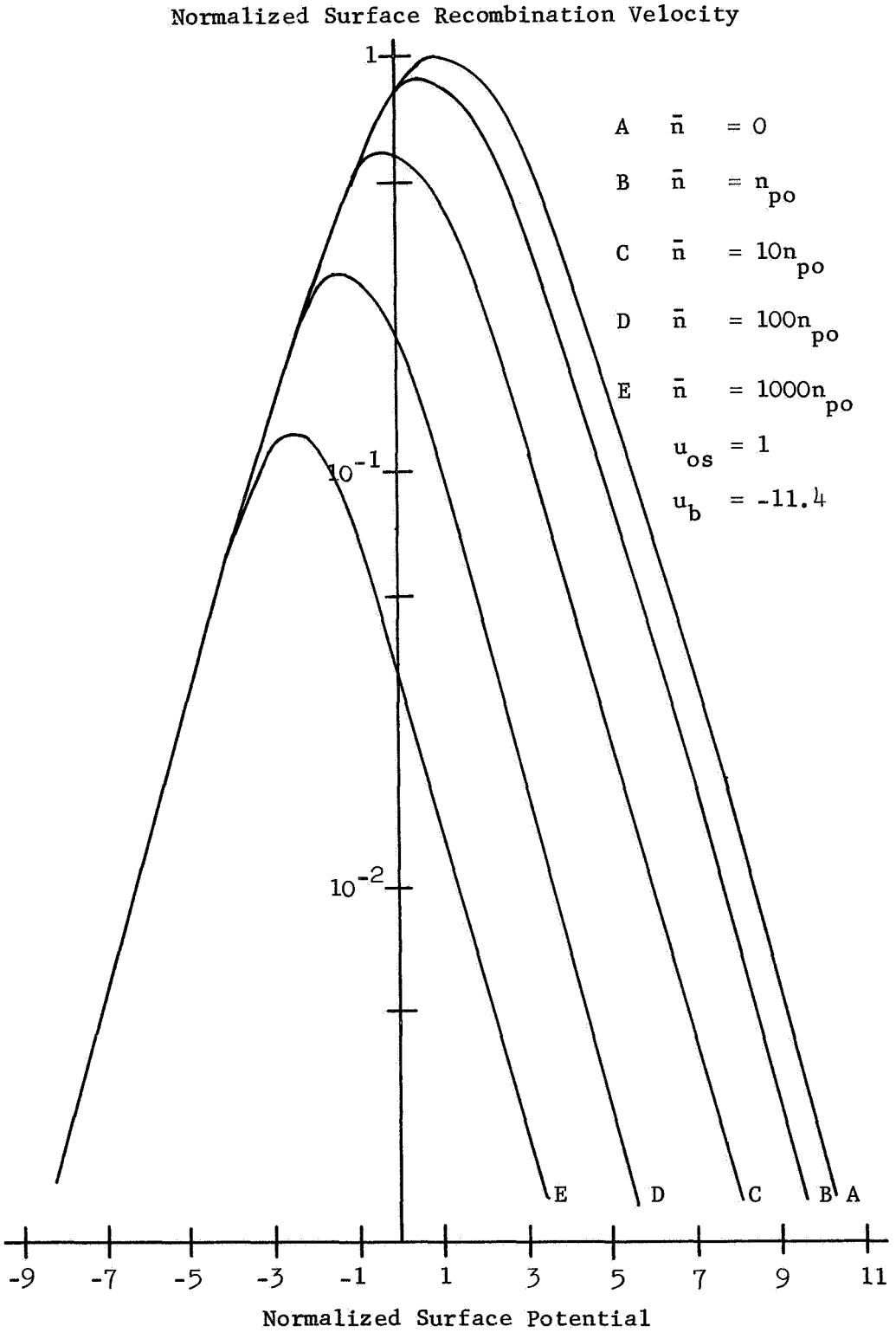

Figure 15 The variation in surface recombination velocity for a uniform recombination center distribution with excess carrier concentration

Simultaneous measurements were made on the completed devices of both MOS capacitance and short circuit current using an experimental arrangement shown in Figure 16. Typical measurements for the MOS solar cell devices are shown in Figures 17 and 18. The capacitance and dissipation factor are typical of those observed on MOS devices. The short circuit current measurements were found to be dependent on the sweep rate as shown in Figure 18. These time variations in the surface recombination velocity were traced to surface leakage over the oxide beyond the edges of the gate resulting in a spreading space charge layer beyond the edges of the gate. This phenomena occured in the depletion and inversion region of the MOS measurements and prohibited accurate data in this region on surface recombination.

From measurements such as those shown in Figure 17 and 18 and from the mathematical model developed, it was possible to determine the surface recombination velocity as a function of surface potential. Typical measurements are shown in Figure 19. The solid curve is a fit of the model to the experimental data. The experimental measurements could not be extended into the inversion space charge region where surface depletion region recombination dominates because of the difficulty mentioned above in obtaining reliable data on short circuit current in this region. As seen in the figure, surface recombination was found to be strongly dependent on surface potential varying from a minimum value near zero to a maximum value ranging from 1×10^4 to 5×10^4 cm/sec.

From the MOS capacitance measurements, the effective surface state density was also determined. The surface state density ranged from 5×10^{11} to 1×10^{12} $cm^{-2}ev^{-1}$. Typical data are shown in Figure 20. The ratio of hole-to-electron capture probabilities at the surface was found to be 44, while the capture cross sections were estimated to be in the 10^{-17} to $10^{-19} cm^2$ range.

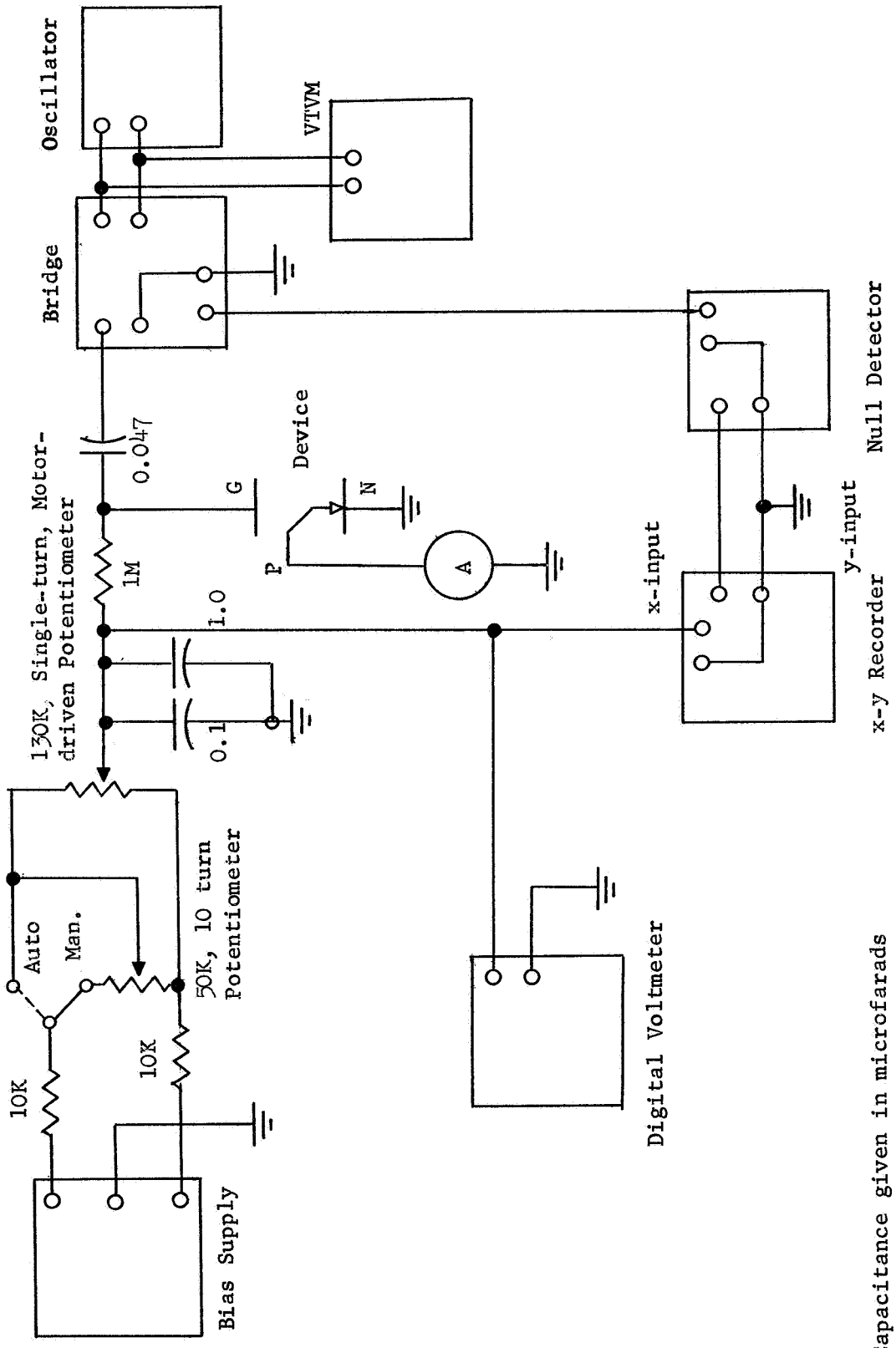

Figure 16 Block diagram of circuit used for measuring MOS capacitance versus gate bias

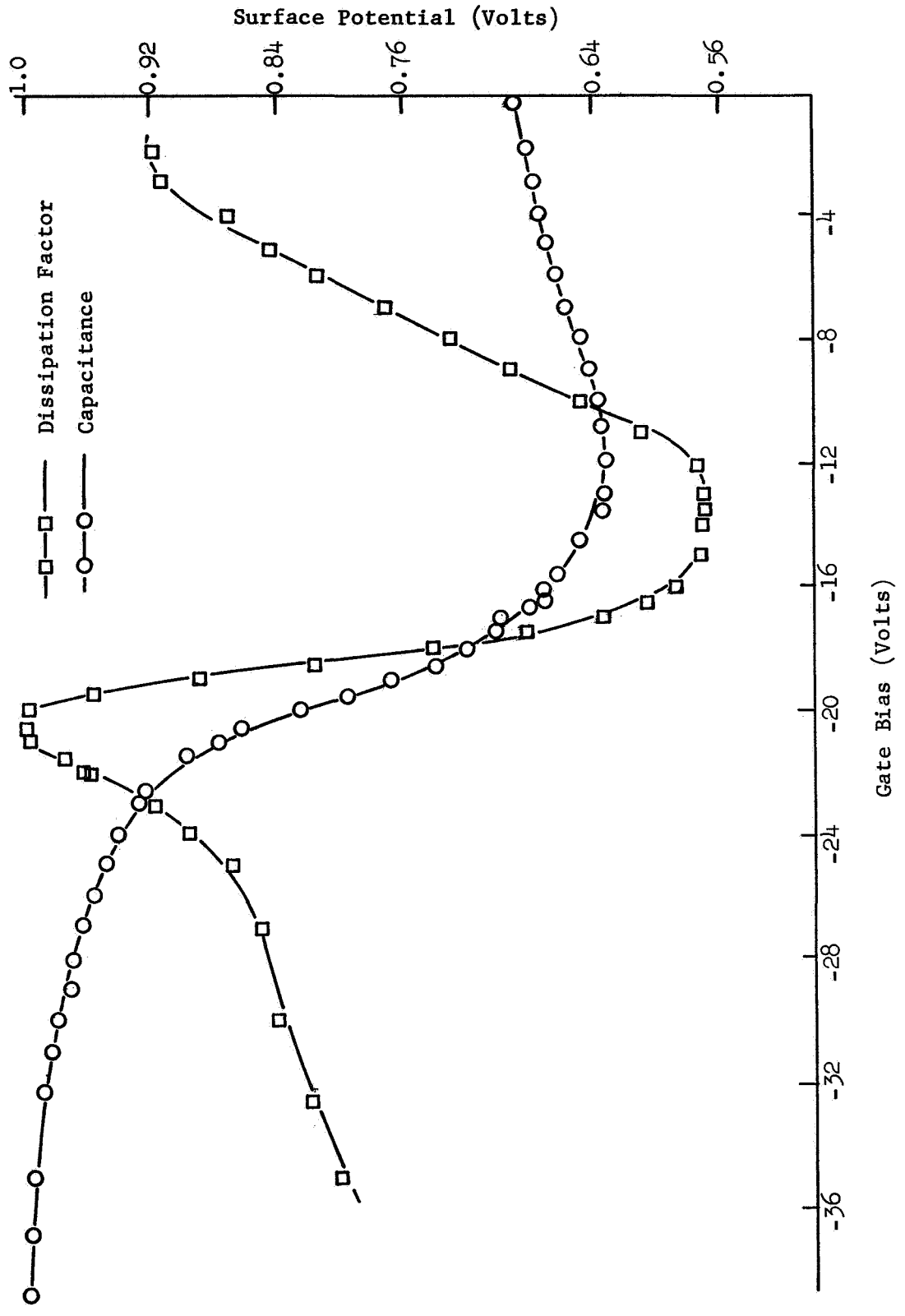

Figure 17 Normalized capacitance and dissipation factor versus gate bias for device no. 9

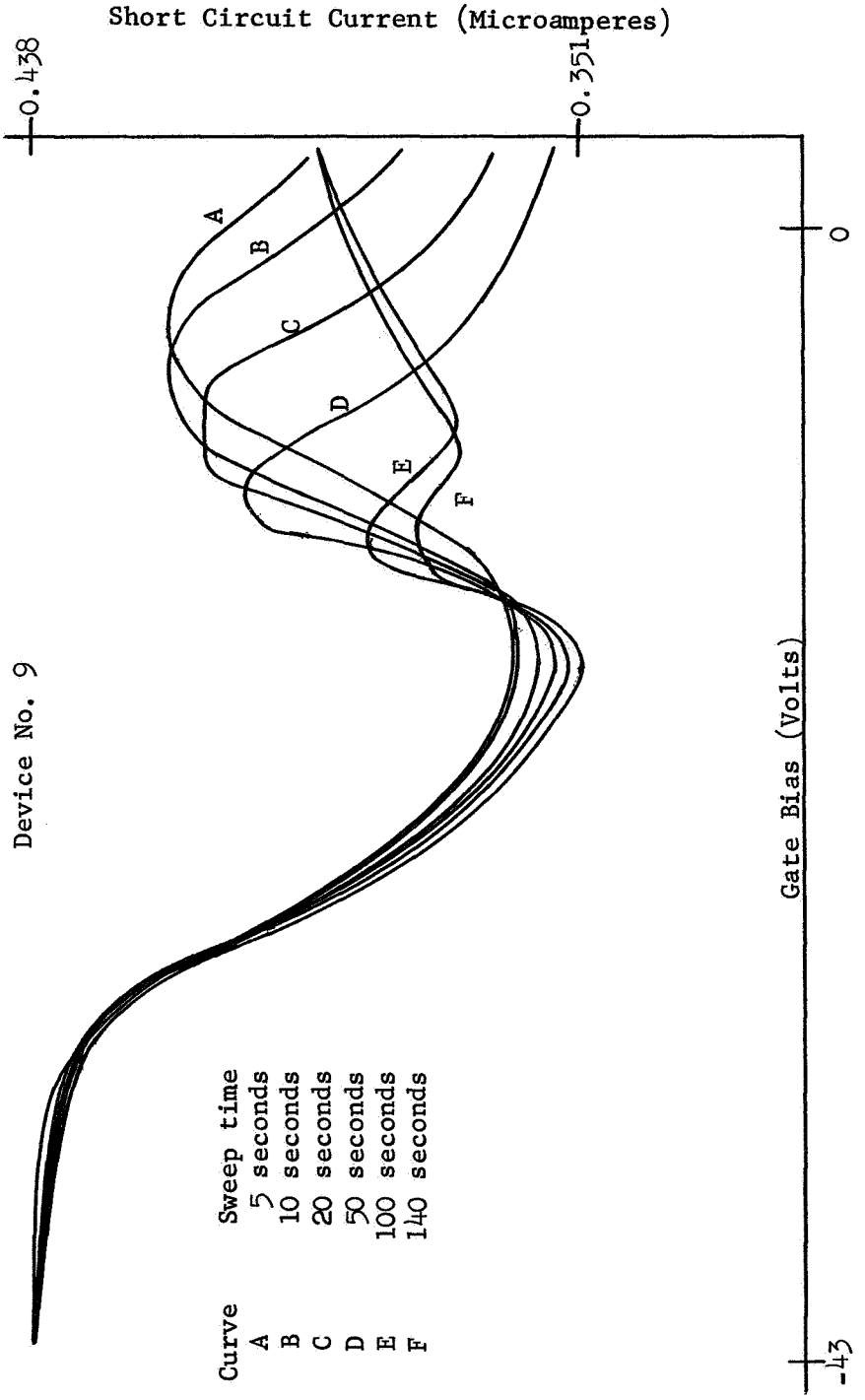

Figure 18 Short circuit current versus dc gate bias for different sweep rates

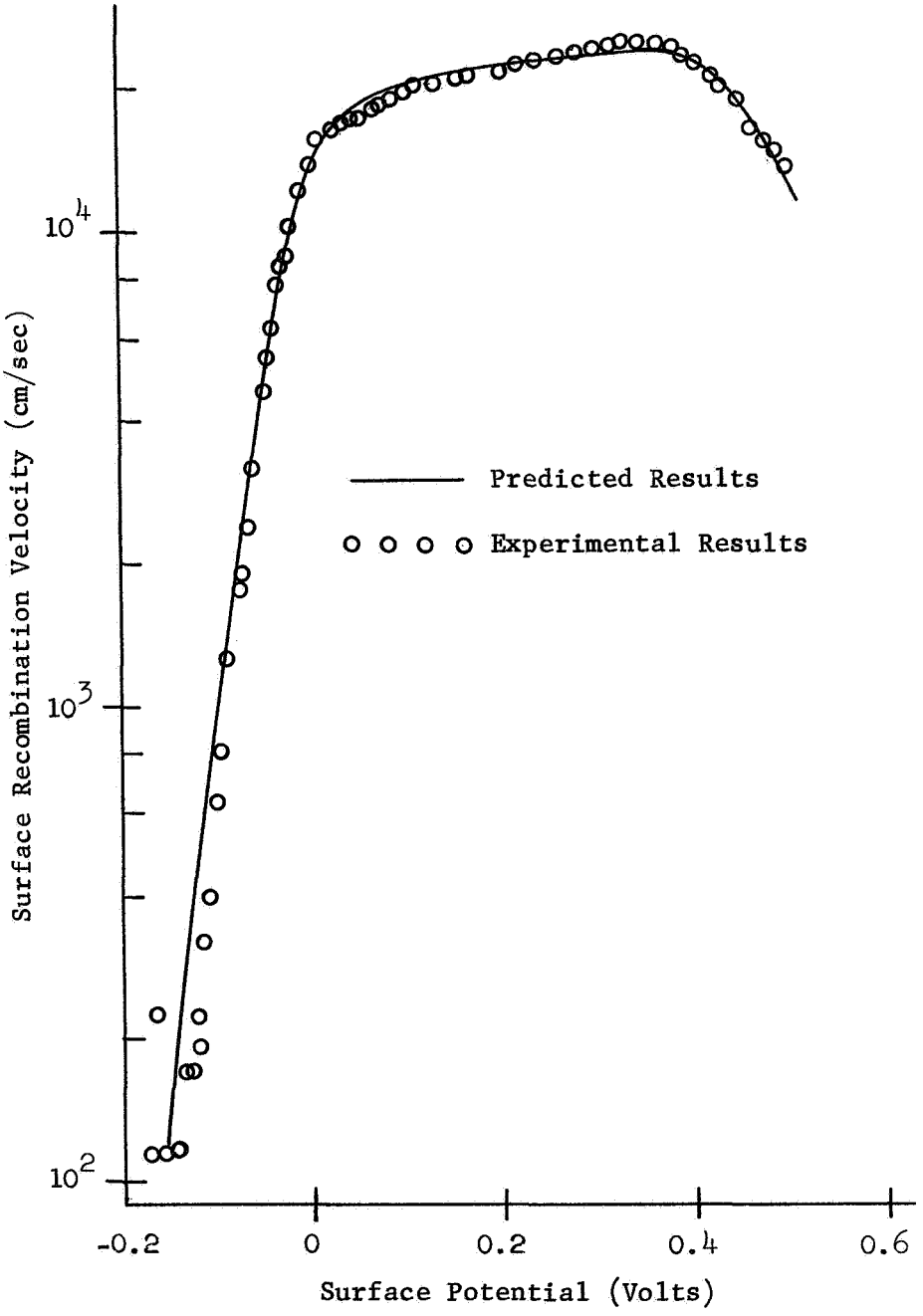

Figure 19 Surface recombination velocity versus surface potential for device no. 42

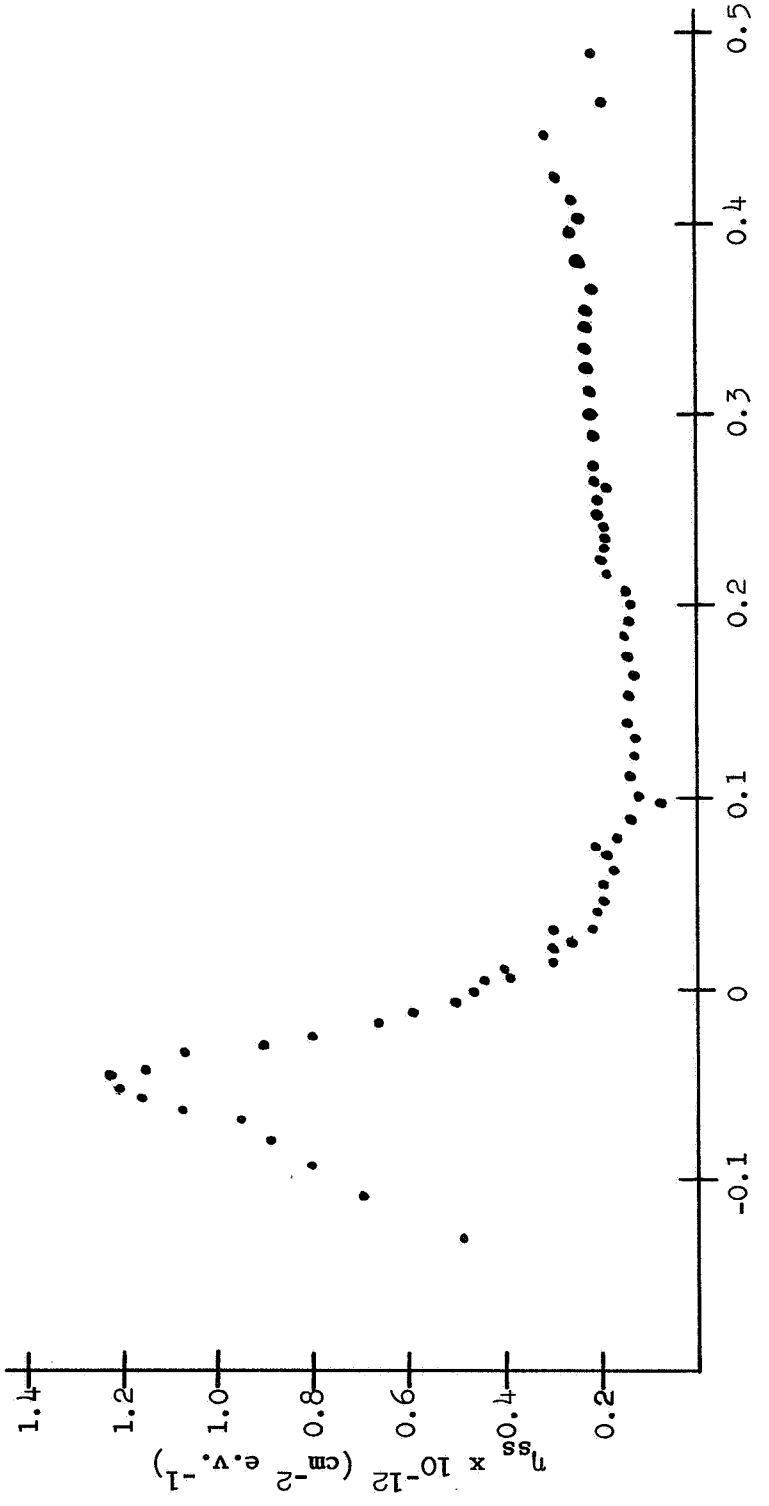

Figure 20 Number of surface states per unit area per unit energy versus surface potential for device no. 9

The original intent of this phase of the research was to develop an experimental technique which could be used to separate out irradiation induced changes in surface recombination due to surface potential changes and those due to an increase in surface recombination state density. It is believed that the present technique has been developed and studied to the point where such measurements can be made. During the course of this work, however, another technique has been reported for making such measurements, and detailed experimental data has been reported on the effect of irradiation on changes in surface recombination levels [13]. The results of this work are essentially that irradiation does increase the density of surface recombination levels and that the increased density of recombination levels is essentially equal to the increased density of surface states from irradiation as obtained from C-V measurements. Because of these measurements which have been reported, detailed measurements on irradiated devices were not made. There appears to be no fundamental reason, however, as to why the MOS solar cell cannot be used to make such measurements. The addition of a gate guard ring can eliminate many of the time dependent effects observed on the devices used in this work.

2.4. Charge Transients in Aluminum-Silicon Nitride-Silicon Capacitors [5] [14]

This phase of the research was initially intended to be an almost identical extension of the work on irradiation effects in steam oxide MOS devices to metal-insulator-silicon capacitors with silicon nitride as the insulating layer. While oxide insulating layers have many desirable features, they do have some undesirable properties. The large mobility of ions in SiO_2 layers and the relatively large irradiation effects are

two such undesirable features. Several other insulators have been investigated in recent years in an attempt to find a more stable and less radiation sensitive material, with silicon nitride being one such material.

The silicon nitride MIS capacitors used in this work were obtained from Texas Instruments while one of the individuals engaged in this research was employed there during the summer. We are indebted to TI for making these devices available for study. The silicon nitride films were pyrolytically deposited on silicon substrates using SiH_4 and NH_3 in an excess hydrogen atmosphere [15] [16]. Thicknesses of the films were in the 1,000 A° range. MIS devices were completed by the filament evaporation of aluminum and mounting on TO-5 headers. Some detectable differences in the films were noted depending on the deposition parameters.

All of the silicon nitride devices tested exhibited rather large room temperature charge instabilities. This was exhibited by a large hysteresis in the C-V plots and by time dependent C-V effects as shown in Figure 21. These C-V curves were recorded on an X-Y recorder by the following procedure:

1. Set the extreme bias points and ground reference point accurately for the motor-driven bias supply.
2. Make at least one complete sweep of the bias, pen up, switching the direction of the trace immediately at each extreme.
3. Stop at the negative extreme and hold, pen up, for 30 seconds. (Negative bias means the aluminum contact is negative).
4. Sweep positive and at the positive extreme immediately switch to negative sweep and lower pen.

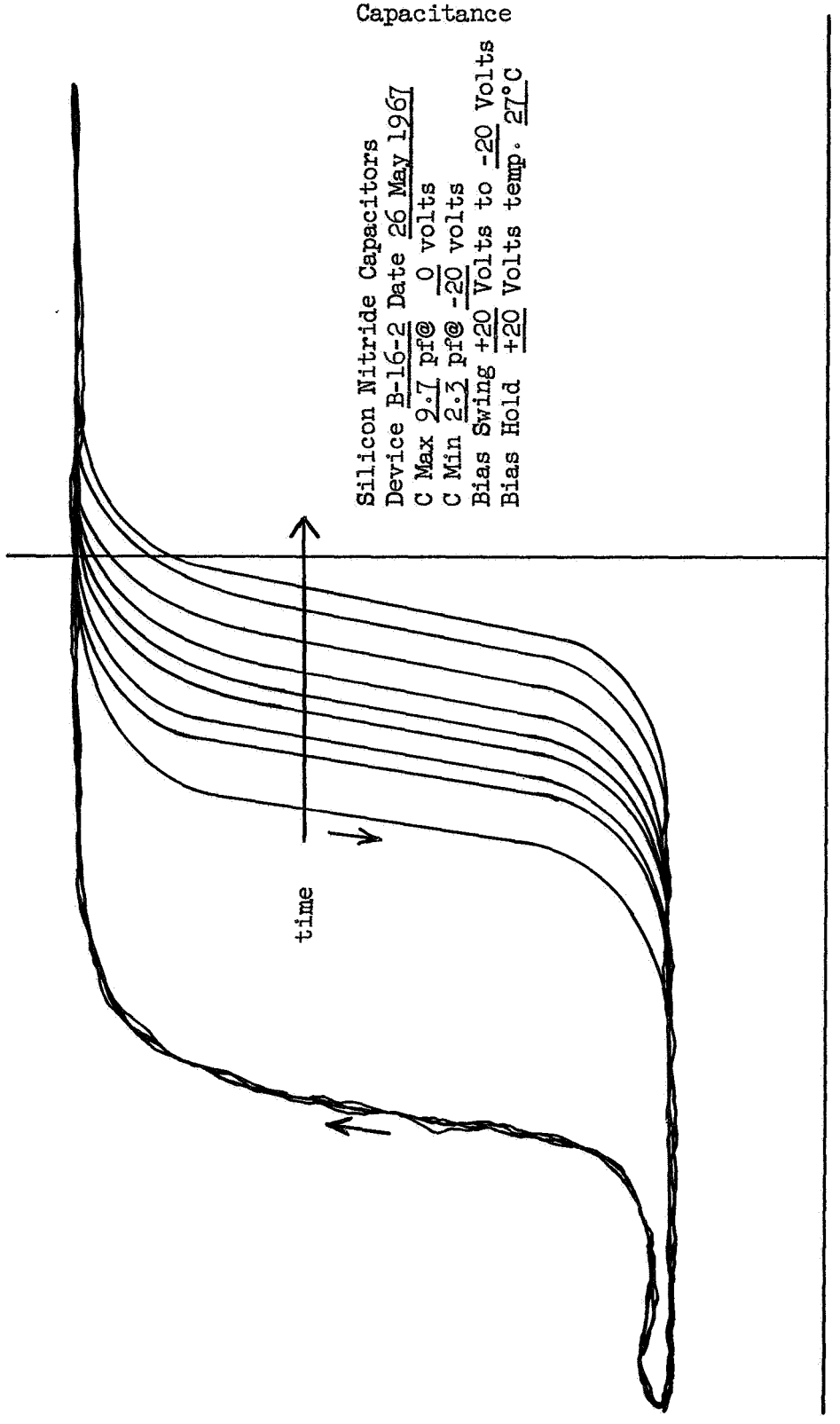

Figure 21 Capacitance vs. voltage recording for capacitor B-16-2. The arrows indicate direction of pen travel

5. At the negative extreme immediately switch to positive sweep with pen down.
6. At positive extreme hold for τ seconds with pen up.
7. Sweep negative, pen down.
8. At negative extreme, switch to positive sweep such that the second (and succeeding) trace falls upon the first positive-going trace (step 5). For longer hold times, this may require a delay of up to a few seconds at the negative extreme.
9. Repeat steps 6 through 8 for longer values of τ.

Since the positive-going trace on the C-V plot is always reproducible, the nitride has the same net positive charge at the beginning of each measurement. Thus each trace represents a separate charge transient measurement for that value of τ. The curves in Figure 21 are for a bias hold of +20 volts and a bias sweep of +20 volts to -20 volts.

The shift in flat band voltage for the C-V curves can be converted into an effective density ΔN_s of charge in the insulator at the insulator-semiconductor interface. Typical values of ΔN_s as a function of the positive bias hold time are shown in Figures 22 and 23 for two different devices. The quantity ΔN_s approximates the total change in carrier density within the insulator. The changes are seen to be on the order of 10^{12} charges/cm^2 for bias hold times between 10 sec and 100 sec.

The rapid changes in insulator charge make it difficult to interpret the experimental results in terms of a physical model. Qualitatively the experimental results can be explained in two ways. The C-V shift with bias for Si_3N_4 is in the opposite direction to that observed for SiO_2. This can only be explained by an electronic type of charge transfer of either electrons or holes across the insulator-semiconductor interface or by a very large density of interface states.

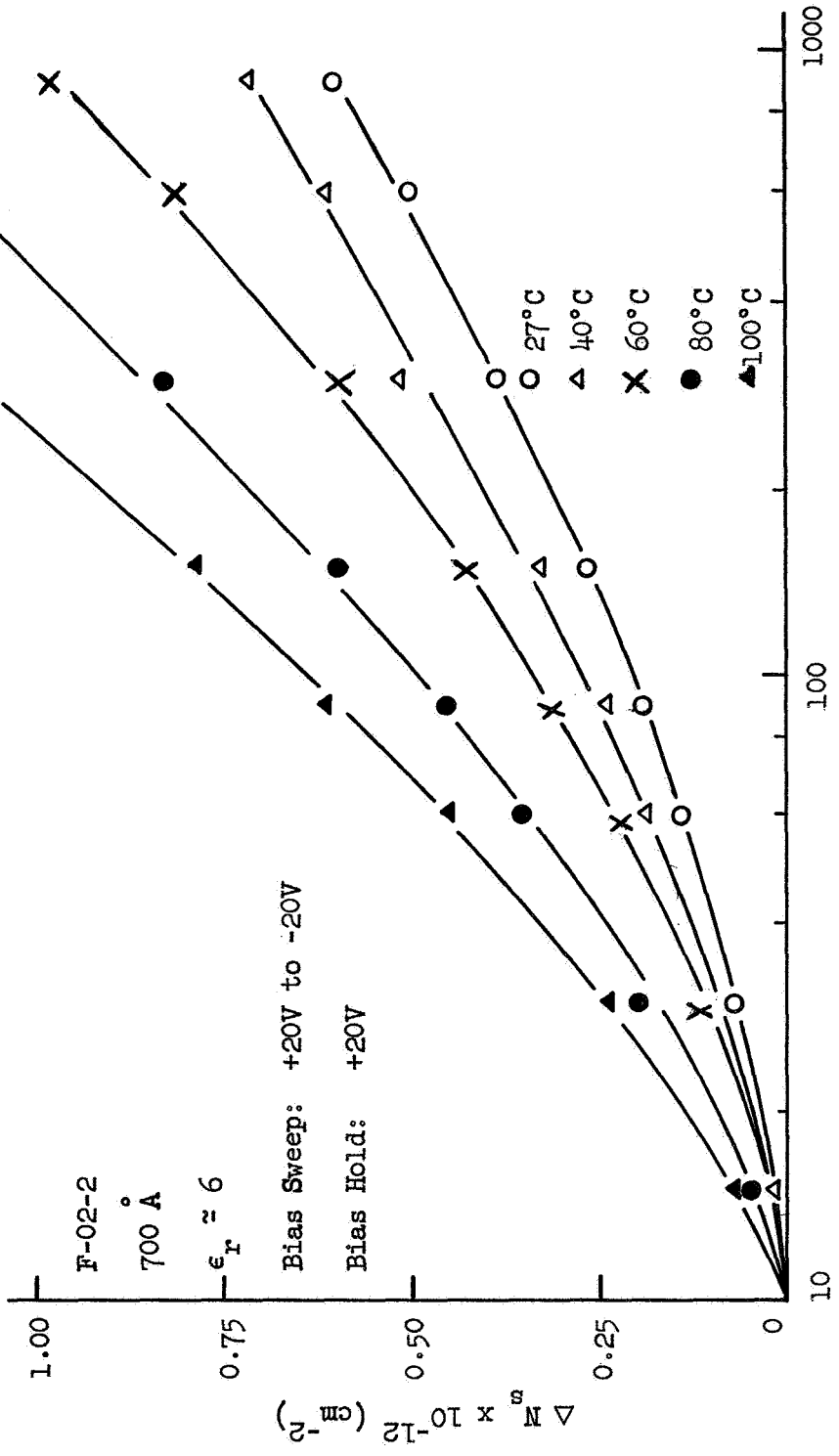

Figure 22 Surface charge density change for capacitor F-02-2

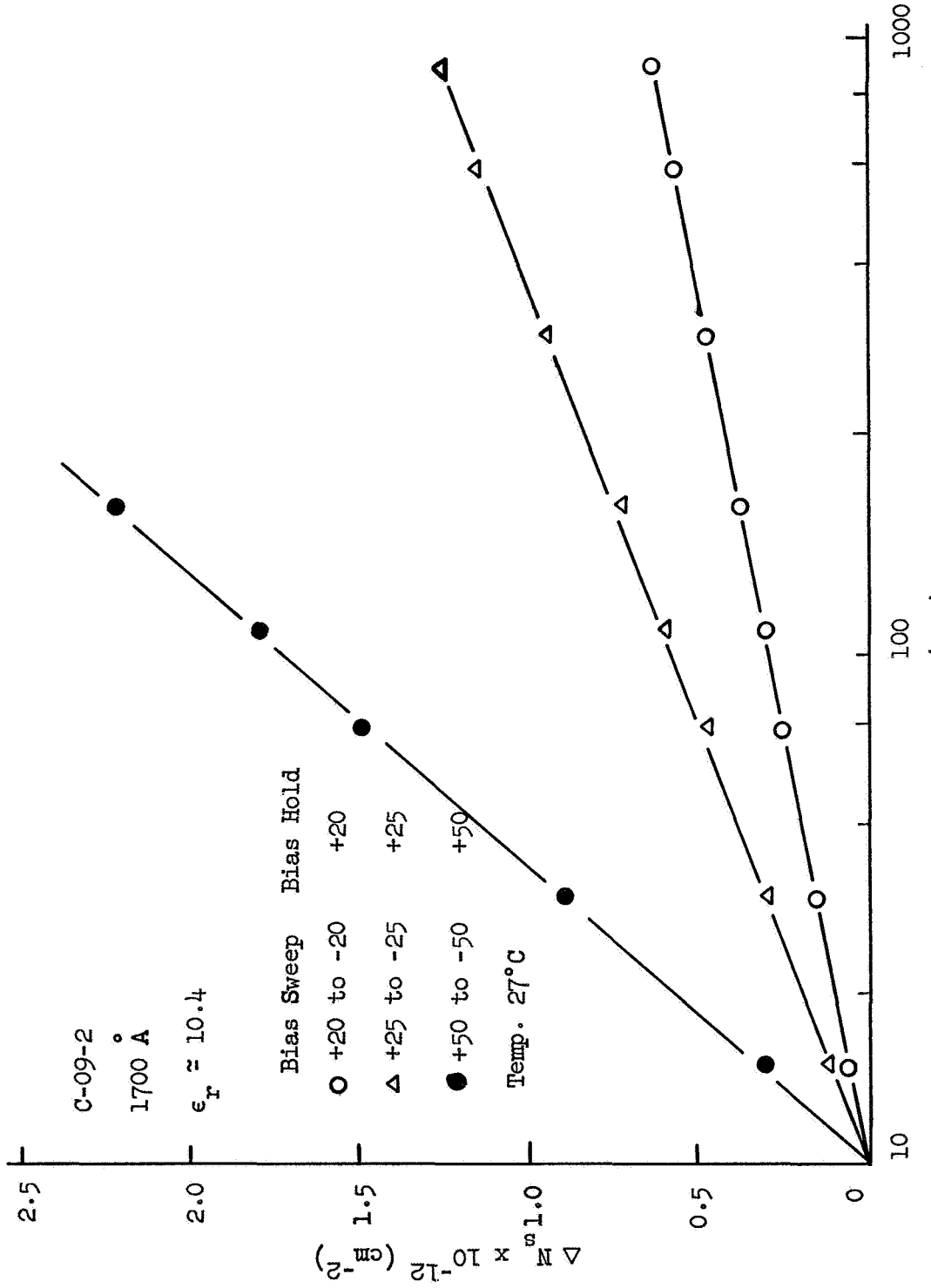

Figure 23 Surface density change vs time for capacitor C-09-2

The model of charge transfer across the interface between the semiconductor and insulator has been studied in some detail in this research. Even assuming this type of charge motion and neglecting surface states there are still two possible models for the observed instability. Either charge is released from traps within the insulator and flows out of the insulator, or charge is injected into the insulator where it subsequently becomes trapped. Both of these possibilities have been studied in this work and were found to predict similar time behaviors. The exact physical model for the instability could not be deduced from the work performed in this phase of the work.

The silicon nitride devices were irradiated with gamma rays for varying time periods up to a total time period of 35 hours. During the irradiation, the gate electrode was shorted to the semiconductor. The capacitors showed no detectable effects of the irradiation. There was no observable structural damage or any change in dielectric constant. Capacitance-voltage measurements similar to those shown in Figure 21 were made both before and after irradiation. Both the initial insulator charge and the charge change were essentially the same as before irradiation. Because of the rapid changes in insulator charge, the irradiation could have been producing an initial change in the insulator charge which was then released or compensated before the actual C-V measurements were made some time later. Within the accuracy of the measurements taken in this work, no gamma irradiation effects were detected. Further irradiation studies were not undertaken since Si_3N_4 is not an attractive insulator for metal-insulator-semiconductor devices unless some means can be found for eliminating the electronic instability.

2.5. Electronic Instabilities in Metal-Insulator-Semiconductor Devices [6]

This research project resulted from the work discussed in the previous section. When the initial attempts were made to study irradiation effects on silicon nitride capacitors, it became aparent that little useful information could be obtained until a more complete understanding of the instability present in these devices was obtained. The previous work showed that the bias dependent changes in insulator charge were opposite to that in SiO_2 films and opposite to that of ion motion within the silicon nitride. Thus a more thorough investigation was undertaken to understand this electronic type of instability in MIS structures.

A study of the various posible type of instabilities in MIS structures shows that the type of instability present with silicon nitride can only arise from electronic type of interface states or from electron and hole injection from the semiconductor into the insulator where the carriers subsequently become trapped. The change in insulator or surface state charge following the application of a bias voltage is found to experimentally depend on time t approximately as ln(t). This behavior is consistent with Schottky barrier injection into the insulator and the subsequent trapping of the carriers. Thus Schottky barrier injection of electrons and holes over relatively low barriers between the silicon nitride and the semiconductor are thought to be responsible for the instability present in silicon nitride films. A model has been developed for this Schottky barrier injection and shown to be in generally good agreement with the experimental data [6].

Typical instabilities present in silicon nitride films are shown in Figure 24, which shows the flat-band voltage of an MIS capacitor following

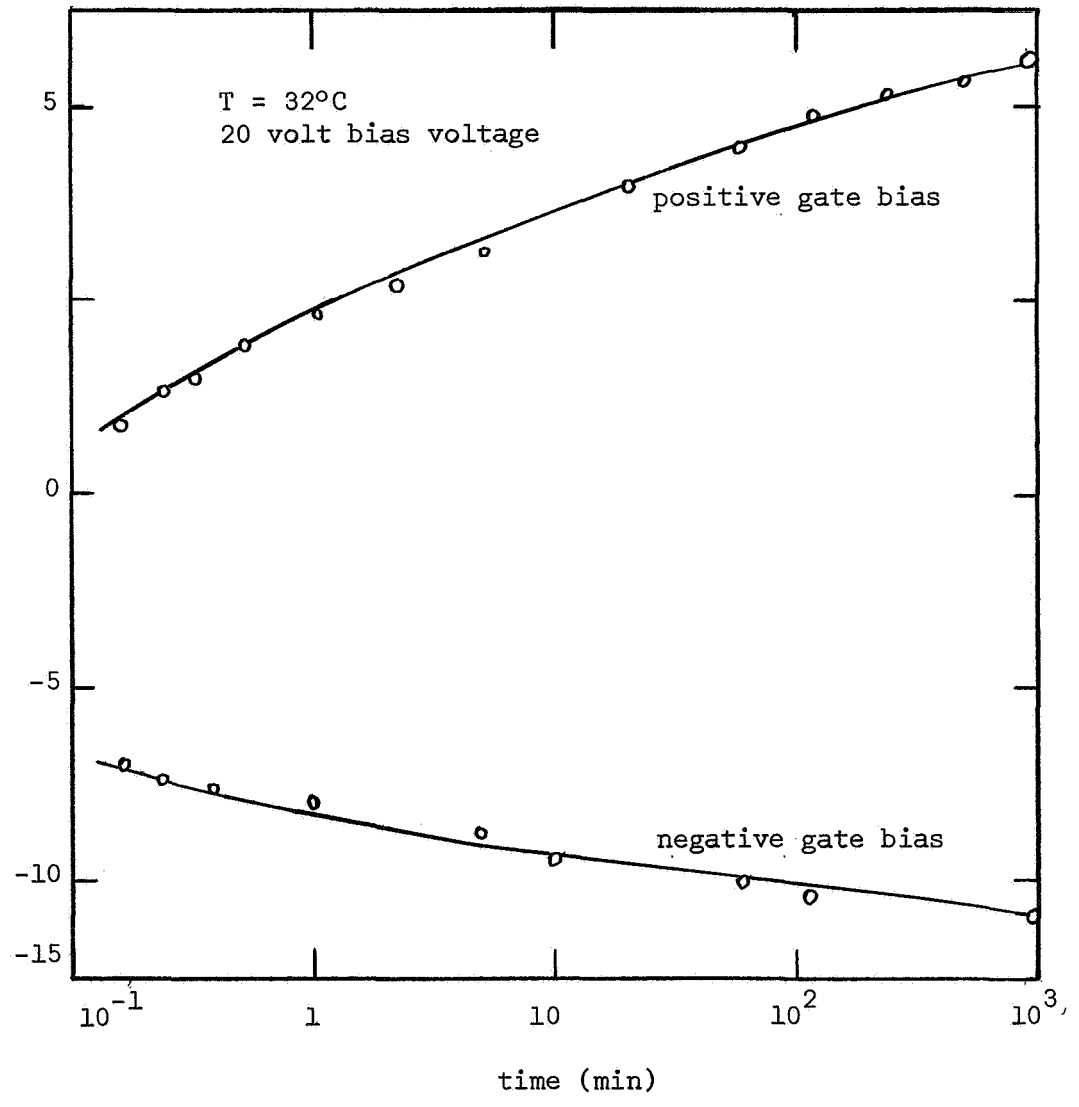

Figure 24. Typical shift in flat-band voltage with time under positive and negative bias for Si_3N_4 devices

the applications of a positive bias voltage and a negative bias voltage. The flat-band voltage was measured by taking fast C-V bias sweeps (50 msec from -25v to +25v) to minimize changes in the device during the C-V sweep. Figures 25 and 26 show similar data for another device compared with the theoretical model. It is seen that significant changes in the flat-band voltage occur over many orders of magnitude in time. As seen in the figures times longer than 10^5sec are normally required at and below room temperature for the instability to reach a steady state following a bias voltage change.

From the experimental measurements and the theoretical model, barrier heights for electron and hole injection into the insulator from the silicon have been estimated as well as an estimation obtained for the total band-gap in the silicon nitride insulator. The barriers for holes and electrons have been found to be about 1.5ev to 2.0ev. The barrier for hole injection was typically found to be a few tenths for an ev smaller than the barrier for electron injection. Variations in the individual electron and hole barriers tended to be somewhat larger than the variations in the total band-gap of the silicon nitride which has been estimated to be 4.2ev $\pm$ 0.2ev. This value of band-gap which is obtained purely from the charge instability measurements is in good agreement with the value of 4.5ev reported from optical measurements [17].

This work on electronic instabilities in MIS devices has shed some light on the important problem of the requirements for charge stable MIS devices. As opposed to ions in the insulator, Schottky barrier injection is an inherent feature of all possible insulator-semiconductor interfaces. Charge instabilities due to Schottky barrier injection can only be eliminated in two ways. Either the trap density in the insulator must be extremely low so very few carriers can become trapped or the barrier must be very high so few carriers are injected into the insulator. The elimination

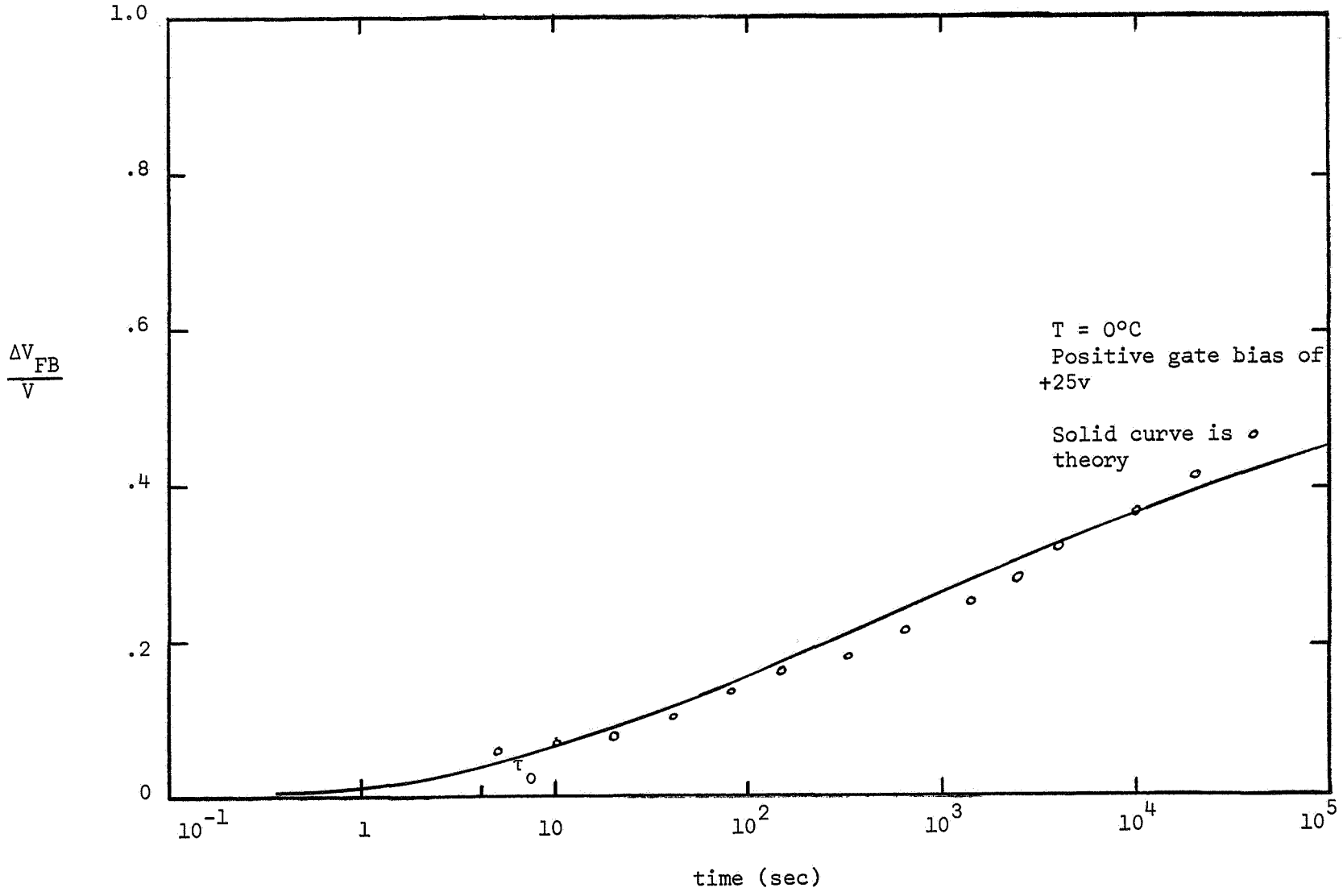

Figure 25. Typical Flat-band voltage shift for positive gate bias.

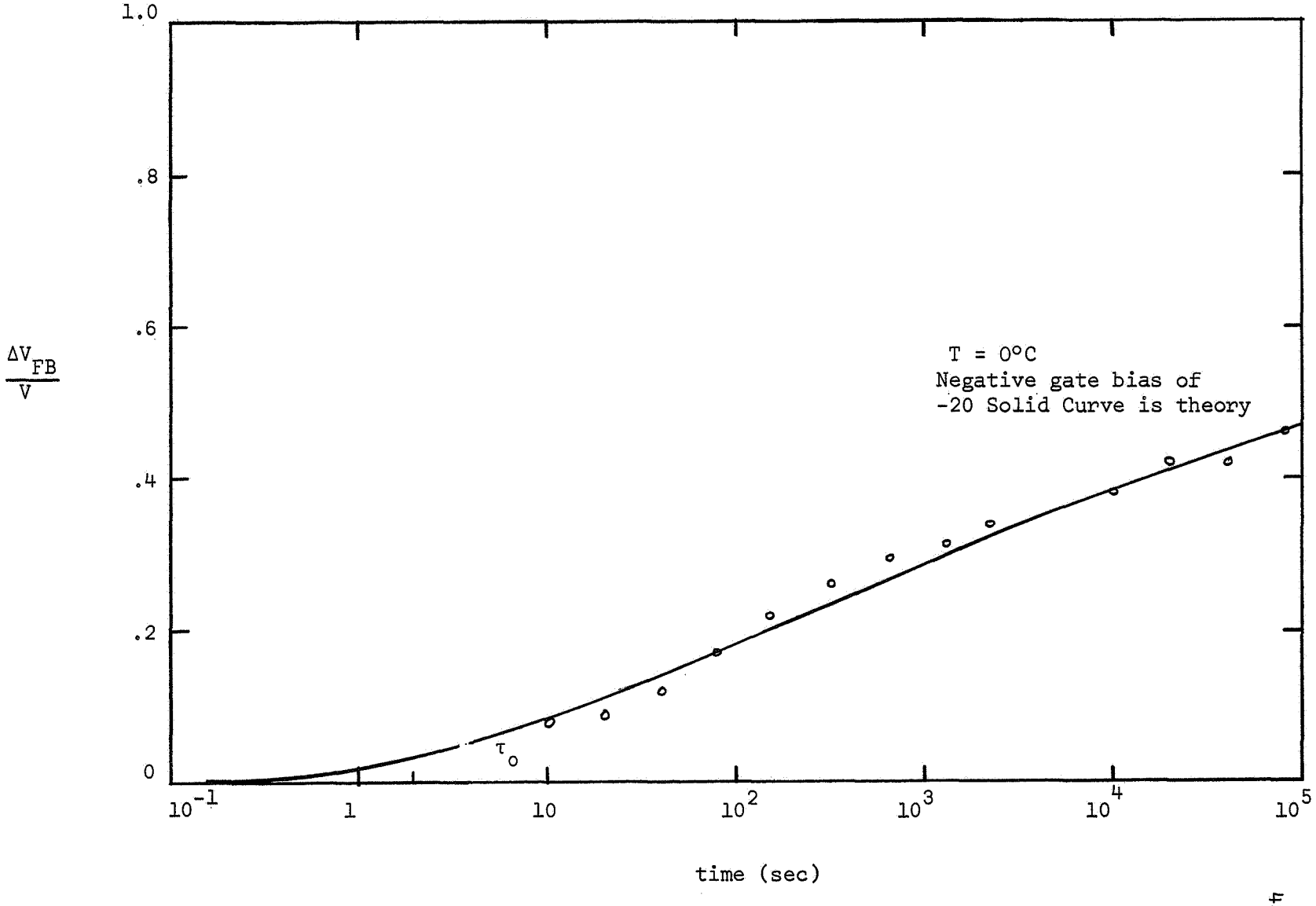

Figure 26. Typical flat-band voltage shift for negative gate bias

of traps does not appear to be feasable with present techniques of depositing or growing insulators. Thus the use of a wide band-gap insulator near the silicon interface appears to be the only acceptable solution to the Schottky barrier, electronic type of instability. This requires an insulator with a band-gap of about 7 ev or larger to minimize Schottky barrier injection at 300°C and for times less than 10^5 sec. Silicon dioxide fortunately has a band-gap of this magnitude and this is probably the reason the electronic type of instability has not been a problem with these devices.

3. Discussion and Conclusions

The research performed during the past four years on this grant has helped to provide a more complete understanding of irradiation effects and in particular of gamma irradiation effects on semiconductor surface and on metal-insulator-semiconductor devices. From the work performed here and by other investigators during the past few years a fairly consistent picture has energed as to irradiation effects on semiconductor surfaces. Practically all semiconductor devices and especially recent devices have some type of insulating layer over the semiconductor which acts as a surface passivation technique and in the case of MIS devices is an integral part of the actual device. Thus in considering irradiation effects on semiconductor surfaces, the question of irradiation effects on the insulating layer becomes of extreme importance in determining the complete effect of the irradiation on the semiconductor.

For silicon with a thermally grown oxide layer, the effects of irradiation have now become pretty well understood—at least qualitatively. Irradiation with either gamma rays or electrons has two major effects. First, there is an increase in the density of electronic states within the energy gap at the insulator-semiconductor interface. This leads to an increase with irradiation of surface recombinations almost directly proportional to the increased surface state density. This also is detected by a distortion of the shape of the C-V characteristic of an MOS device. The second major effect of irradiation is a change in the charge within the oxide. This is normally an increase in the positive charge within the oxide. This is believed to be due to the creation of electron-hole pairs within the oxide with the trapping of essentially all of the holes while

many of the electrons are able to get out of the oxide. This effect is greatly enhanced by the presence of a bias voltage during irradiation which aids in removing the created electrons. This charge can be annealed out at elevated temperatures, but because of the fairly deep hole traps, the charge can remain essentially constant at room temperature for long periods of time. The changes in oxide charge are reflected in the semiconductor by changes in the surface potential at the semiconductor surface, and consequently in such surface properties as surface recombination.

The experimental and theoretical studies undertaken in this work have helped to verify the above general picture and to give detailed information on gamma irradiation effects on silicon surfaces. In particular the studies of irradiation on steam grown SiO_2 MOS structures have shown the increases in interface states as well as the irradiation induced changes in oxide charge. The study of surface recombination in irradiated silicon has illustrated the influence of irradiation induced changes in surface potential on surface recombination and shown the necessity for knowing the surface potential in order to properly interpret surface recombination data. In addition a new technique was developed for simultaneously measuring both surface potential and surface recombination. This technique makes use of a combined MOS device and a solar cell.

The major features of irradiation on semiconductors with insulators other than thermally grown oxides are expected to be similar to those of the oxides. Attempts however to perform similar studies on silicon nitride insulated silicon have led to difficulties because of the room

temperature charge instabilities present with these films. This instability has been found to be entirely different from the ionic instability found in oxide devices. This has been studied in detail and is believed to be due to Schottky barrier injection of electrons and holes into the nitride film from the silicon. A model explaining this effect has been developed and some of the consequences of this phenomena on building stable irradiation insensitive devices have been discussed.

The major effects of irradiation on semiconductor surface properties are now fairly well understood. The remaining tasks concern how to use this information to improve the properties of semiconductor devices which must operate in an irradiation environment. The most pressing need is the development of an insulator passivation technique which does not show a large build-up of charge under irradiation. This will probably be a multilayered insulator with thermally grown SiO_2 as the insulator near the silicon interface. There is a wide choice of insulators to use in combination with SiO_2 and many of these are just beginning to be investigated.

REFERENCES

1. R. D. Evans, The Atomic Nucleus, McGraw-Hill Book Co., Inc., New York (1955) p. 712.

2. R. J. Mattauch and R. W. Lade, "A Study of the Effects of Co^{60} γ-Radiation on Steam-Grown SiO_2 MOS Structures", Electrical Engineering Dept., N. C. State University, Semiconductor Device Laboratory Report SDL-5-588-1, 1966.

3. M. A. Littlejohn and R. W. Lade, "Influence of Co^{60} Gamma Irradiation on the Bulk and Surface Recombination Rates in Silicon", Electrical Engineering Dept., N. C. State University, Semiconductor Device Laboratory Report SDL-6-588-1, 1967.

4. F. J. Morris and R. W. Lade, "A Study of the Effects of Surface Potential on the Surface Recombination Velocity at a Silicon-Silicon Oxide Interface", Electrical Engineering Dept., N. C. State University, Semiconductor Device Laboratory Report SDL-7-588-1, 1967.

5. C. L. Hutchins and R. W. Lade, " Charge Transients in Aluminum-Silicon Nitride-Silicon Capacitors", Electrical Engineering Dept., N. C. State University, Semiconductor Device Laboratory Report SDL-8-588-1, 1968.

6. J. R. Hauser and J. R. Bridges, "Electronic Instabilities in Metal-Insulator-Semiconductor Devices", Electrical Engineering Dept., N. C. State University, Semiconductor Device Laboratory Report SDL-9-588, 1968.

7. R. J. Mattauch and R. W. Lade, "Surface state density variations on MOS structures due to gamma radiation," Proc. IEEE, vol. 53, p. 1748, 1965.

8. E. H. Snow, A. S. Grove, B. E. Deal, and C. T. Sah, "Ion Transport Phenomena in Insulating Films", J. Appl. Phys., vol. 36, pp. 1664-1673, 1965.

9. E. Yon, W. H. Ko, and A. B. Kuper, "Sodium distribution in thermal oxide on silicon by radiochemical and MOS analysis," IEEE Trans. Electron Devices, vol. ED-13, pp. 276 - 280, 1966.

10. K. H. Zaininger and G. Warfield, "Limitations of the MOS capacitance method for the determination of semiconductor surface properties," IEEE Trans. Electron Devices, vol. ED-12, pp. 179-193, 1965.

11. B. E. Deal, M. Sklar, A. S. Grove, and E. H. Snow, "Characteristics of the surface-state charge (Q_{ss}) of thermally oxidized silicon," J. Electrochem. Soc, vol. 114, pp. 266-274, 1967.

12. M. A. Littlejohn and R. W. Lade "Influence of Co^{60} Gamma Irradiation on the Surface and Bulk Recombination Rates in Silicon," IEEE Trans. on Nuclear Science, vol NS-14, pp. 305-318, 1967.

13. D. J. Fitzgerald and A. S. Grove, "Radiation-induced increase in surface recombination velocity of thermally oxidized silicon structures," Proc. IEEE, vol. 54, pp. 1601-1602, 1966.

14. C. L. Hutchins and R. W. Lade, "Charge Storage in Metal-Silicon Nitride-Silicon Capacitors", Proc. IEEE, vol. 55, p. 1494, 1967.

15. V. Y. Doo, D. R. Nichols, and G. A. Silvey, "Vapor deposition of silicon nitride," 1965 Fall Meeting of Electrochem. Soc., Buffalo, N. Y., Recent News Paper.

16. V. Y. Doo and D. R. Nichols, "Effect of various composition reactants on pyrolytic silicon nitride films," 1966 Fall Meeting of Electrochem. Soc., Philadelphia, Pa., Abstract 146.

17. P. V. Gray, Paper presented at the Silicon Interface Specialists Conference, March 1-3, 1967, Las Vegas, Nev.